MASTERARBEIT | MASTER'S THESIS

Titel | Title

Leaching of organic rubber-derived compounds from road and climbing hall dust into simulated lung fluids

verfasst von | submitted by

Emily Alice Roche B.Sc.

angestrebter akademischer Grad | in partial fulfilment of the requirements for the degree of

Master of Science (MSc)

Wien | Vienna, 2025

Studienkennzahl lt. Studienblatt | Degree programme code as it appears on the student record sheet:	UA 066 299
Studienrichtung lt. Studienblatt | Degree programme as it appears on the student record sheet:	Masterstudium Environmental Systems: Processes - Pollution - Solutions
Betreut von | Supervisor:	Univ.-Prof. Dr. Thilo Hofmann

Acknowledgements

First of all, I'd like to thank my supervisor, Prof. Dr. Thilo Hofmann, for making this project possible and for his guidance, helpful comments, and discussions throughout the process.

A big thank you to my mentor, Dr. Anya Sherman, who was always incredibly supportive — from helping me with basics in the lab to always being open to so many productive discussions. Your positivity and love for the project really motivated me, and I'm very grateful for that.

I'd also like to thank the department of Prof. Dr. Lea Ann Dailey, Dr. Gabriela Hädrich for letting me use the NGI (and for tolerating my dirty dust samples), and Lukas Wimmer for his help and advice with the instrument.

Finally, I want to thank the whole EDGE team for being so welcoming and helpful. I really enjoyed being part of the group.

Abstract

Tire wear particles generated through the mechanical abrasion of tires are released into the environment, where rubber-derived compounds can leach. These compounds, along with their transformation products, are increasingly detected in aquatic systems, soil and air, raising environmental and ecotoxicological concerns. Similar processes of abrasion, diffusion, and transformation are occurring in indoor climbing gyms, likely originating from the rubber soles of climbing shoes. Given the potential for humans to inhale these airborne particles, it is important to evaluate the leaching behavior of rubber-derived compounds in the lungs. This study investigated the leaching of 16 rubber-derived compounds from road and climbing hall dust in simulated lung fluids. Samples were fractionated with the Next Generation Pharmaceutical Impactor to isolate respirable particles (D50 $\leq$ 4.42 µm). Dust was characterized using Scanning Electron Microscopy and extracted with Accelerated Solvent Extraction, confirming the presence of rubber-derived compounds in the respirable fraction. Leaching experiments were conducted using simulated epithelial lung fluid and phagolysosomal fluid, the latter tested both with and without hydrogen peroxide to mimic the oxidative environment of the phagolysosome. Leaching was assessed over 7 days in simulated epithelial lung fluid and two hours in phagolysosomal fluid, and leachates were analyzed using Liquid Chromatography coupled to Triple Quadrupole Mass Spectrometry. Additionally, stability experiments were performed to evaluate the persistence of these compounds in the lung fluids. Results showed a rapid initial release of compounds in all fluids, with slower increases only observed over 7 days in simulated epithelial lung fluid. The presence of hydrogen peroxide enhanced the degradation of certain parent compounds, such as 2-mercaptobenzothiazole, while simultaneously increasing concentrations of their transformation products, such as 2-hydroxybenzothiazole and benzothiazole. These findings reveal that oxidative conditions in the lung may alter the bioaccessibility and transformation of rubber-derived compounds. This study revealed the leaching of rubber-derived compounds from airborne dust into simulated lung fluids. Since the toxicity of these compounds to humans remains largely unknown, future research should focus on identifying possible health risks following respiration of rubber-derived compounds.

Kurzfassung

Reifenabriebpartikel, die durch die mechanische Abnutzung von Reifen entstehen, gelangen in die Umwelt, wo Gummiadditive freigesetzt werden können. Diese Chemikalien sowie ihre Transformationsprodukte werden zunehmend in Gewässern, Böden und in der Luft nachgewiesen, was zu umwelt- und ökotoxikologischen Bedenken führt. Ähnliche Prozesse des Abriebs, der Diffusion und der Transformation finden auch in Kletterhallen statt und gehen vermutlich von den Gummissohlen von Kletterschuhen aus. Da Menschen die Partikel in der Luft einatmen können, muss das Freisetzungsverhalten dieser Chemikalien in der Lunge untersucht werden. In dieser Studie wurde die Freisetzung von 16 Gummiadditiven und deren Transformationsprodukten aus Straßen- und Kletterhallenstaub in simulierten Lungenflüssigkeiten untersucht. Mithilfe des Next Generation Pharmaceutical Impactor wurden Staubproben in einatembare Partikelgrößen fraktioniert (D50 $\leq$ 4,42 µm). Die Staubproben wurden mittels Rasterelektronenmikroskopie charakterisiert und mit beschleunigter Lösungsmittelextraktion auf das Vorkommen der Chemikalien untersucht. Die Experimente erfolgten in simulierter epithelialer Lungenflüssigkeit sowie in phagolysosomaler Flüssigkeit. Letztere wurde mit und ohne Zugabe von Wasserstoffperoxid getestet, um die oxidativen Bedingungen im Phagolysosom nachzubilden. Die Freisetzung der Stoffe wurde über einen Zeitraum von sieben Tagen (in simulierter epithelialer Lungenflüssigkeit) bzw. zwei Stunden (in phagolysosomaler Lungenflüssigkeit) beobachtet und mittels Triple-Quadrupol-Flüssigchromatographie-Massenspektrometrie gemessen. Zusätzlich wurde die Stabilität der Chemikalien in den Lungenflüssigkeiten untersucht. Die Ergebnisse zeigten in allen Flüssigkeiten eine rasche Anfangsfreisetzung, wobei in der simulierten epithelialen Lungenflüssigkeit über die Zeit ein langsamer Konzentrationsanstieg beobachtet wurde, während die Konzentration in der phagolysosomalen Flüssigkeit weitgehend konstant blieb. Unter den oxidativen Bedingungen der phagolysosomalen Flüssigkeit kam es zu verstärktem Abbau bestimmter Chemikalien, wie zum Beispiel 2-Mercaptobenzotiazol, während gleichzeitig erhöhte Konzentrationen seiner Transformationsprodukte 2-Hydroxybenzotiazol und Benzotiazol gemessen wurden. Dies deutet darauf hin, dass oxidative Prozesse in der Lunge die Verfügbarkeit und Umwandlung von Gummizusatzstoffen und ihrer Transformationsprodukte maßgeblich beeinflussen können. Die Studie zeigt die potenzielle Freisetzung dieser Chemikalien in simulierten Lungenflüssigkeiten. Da die Toxizität der Stoffe für den Menschen noch weitgehend unklar ist, sollten zukünftige Studien sich darauf konzentrieren mögliche Gesundheitsrisiken nach dem Einatmen dieser Chemikalien zu klären.

Contents

List of Tables

List of Figures

Abbreviations

2OH-BTZ 2-hydroxybenzothiazole.

2SH-BTZ 2-mercaptobenzothiazole.

2amino-BTZ 2-aminobenzothiazole.

5methyl-BTR 5-methyl-1H-benzotriazole.

6PPD N-(1,3-dimethylbutyl)-N'-phenyl-p-phenylenediamine.

6PPDQ N-(1,3-dimethylbutyl)-N'-phenyl-p-phenylenediamine-quinone.

BTZ benzothiazole.

CPPD N-cyclohexyl-N'-phenyl-p-phenylenediamine.

CPPDQ N-cyclohexyl-N'-phenyl-p-phenylenediamine-quinone.

d4-BTZ d4-benzothiazole.

d5-6PPDQ d5-6PPD-quinone.

DPG 1,3-diphenylguanidine.

DPPC dipalmitoylphosphatidylcholine.

DPPD N,N'-diphenyl-p-phenylenediamine.

DPPDQ N,N'-diphenyl-1,4-phenylenediamine-quinone.

H_2O_2 hydrogen peroxide.

HMMM hexa(methoxymethyl)melamine.

IPPD N-isopropyl-N'-phenyl-p-phenylenediamine.

IPPDQ N-isopropyl-N'-phenyl-p-phenylenediamine-quinone.

PPDs N,N'substituted p-phenylenediamines.

PSF phagolysosomal fluid.

SEM Scanning Electron Microscopy.

SLF simulated epithelial lung fluid.

TRWP Tire and Road Wear Particles.

1. Introduction

While plastic as a mass-produced material was only invented in the early 20th century, it has become an integral part of everyday life. In many applications, plastic is superior to traditional materials due to its durability, flexibility, and low production costs [1]. Plastics are generally divided into two major categories: thermosets and thermoplastics. While rubber is technically an elastomer rather than a plastic, it is often grouped with plastics [1, 2]. For instance, in EU regulations and policies tire wear particles are considered to be a large source of microplastic in the environment [3, 4]. Global plastic production has increased immensely, from around 20 million tonnes in the 1950s to more than 400 million tonnes in 2022 [5]. From food packaging to construction and clothing, plastic is found in many different applications. However, only about 9 % of all plastic produced has been recycled, while approximately 12 % has been incinerated. The vast majority of plastic waste, if not still in use, ends up in landfills or the environment [6].

Unfortunately, the very durability that makes most plastic so useful also means it can persist in the environment for generations [1]. Its persistence, along with the continuous accumulation, raises concerns about long-term effects on ecosystems and human health. Among these pollutants, tire wear particles represent a significant source of microplastic emissions, particularly in urban areas with high traffic density. It is estimated that around 3-7 % of particulate matter with aerodynamic diameter of 2.5 µm ($PM_{2.5}$) originates from tire wear [7]. As tires degrade through abrasion, they release fine particulate matter containing rubber-derived compounds, some of which are environmentally persistent and potentially hazardous. Studies estimate that approximately 6.1 million tonnes of tire wear particles are emitted globally each year [1, 8].

With the rising number of vehicles on the roads, non-exhaust emissions from tire and brake wear are expected to grow further in the coming years. Moreover, since electric vehicles are generally heavier than conventional cars, the increased friction with the road surface may lead to even greater tire wear emissions [9, 10]. Non-exhaust emissions have only recently become subject to stricter regulation. Regulation No. 117 of the United Nation Economic Commission for Europe (UNECE), in force since 2016, covers multiple aspects of tire safety and performance, such as noise and rolling resistance [11]. The EURO 7 regulation [12], adopted by the European Union in 2024, establishes a legal framework for limiting microplastic emissions from tires. According to EURO 7, by September 2025, UNECE Regulation No. 117 is expected to include limits on tire abrasion for passenger cars, with provisions for heavier vehicles anticipated in 2026 and 2027. Following this, EURO 7 mandates that tire abrasion limits for

new passenger cars will come into force by 2028. These regulations aim to reduce pollution from tire and road wear particles (TRWP) by imposing limits based on the weight of particles emitted per kilometer per ton of vehicle load. As a result, tire manufactures will be required to adapt the composition and manufacturing processes of their products accordingly [13].

Tire wear particles can enter freshwater systems, oceans, and terrestrial environments through road runoff. Particles can also become airborne and are transported through the atmosphere where they can be deposited in remote regions. Modeling studies by Evangeliou et al. suggest that microplastics from tire and brake wear exhibit high transport efficiency and are likely to be deposited in the world's oceans and Arctic regions [8]. As a result, increasing amounts of rubber-derived compounds are being released into the environment, polluting both urban and remote areas. In cities, humans may inhale or ingest these chemicals. While some compounds in rubber have been shown to be toxic to aquatic organisms, their potential health effects on humans via inhalation or ingestion remain largely unknown. Since tire wear products contain a complex mixture of organic compounds — some of which have already been detected in human blood and urine [14, 15] — understanding their leaching potential and chemical stability in biological fluids is essential for assessing possible health risks.

This thesis investigates the leaching behavior of selected rubber-derived compounds under simulated biological conditions, aiming to provide insight into their bioaccessibility and potential for human exposure. By examining their leaching and stability in simulated lung fluids that mimic key inhalation and exposure pathways, this study contributes to a more comprehensive understanding of the fate of rubber-derived compounds in the human body. These findings will help inform future research on the impact of tire wear particles on human health, thereby bridging the gap between existing research on environmental contamination and toxicological risk assessment.

2. State of Knowledge and Aims and Hypotheses

2.1. Rubber and its additives

2.1.1. Composition of Tires

Car tires consist of a complex blend of functionalized rubber and performance-enhancing additives. These include antioxidants (N,N'substituted p-phenylenediamines (PPDs)), crosslinking agents (e.g., hexa(methoxymethyl)melamine (HMMM)), vulcanization accelerators (e.g., 1,3-diphenylguanidine (DPG) and benzothiazole (BTZ)), and corrosion inhibitors (e.g., 5-methyl-1H-benzotriazole (5methyl-BTR)). [16, 17] Many of these added compounds are toxic and pose risks to humans and wildlife [18, 19]. The compounds studied in this research, along with their chemical structures and functions in tires are detailed in Table 2.1.

2.1.2. Emission Pathways

The frictional contact of tires with the road causes the abrasion of rubber particles. Once released, these particles accumulate on road surfaces, where they can undergo further environmental transformation [9]. Additionally, road surfaces can degrade and release mineral particles, which combine with tire-wear particles and build composites that are collectively referred to as tire and road wear particles (TRWP) [9, 10]. Therefore, settled road dust can contain particles from multiple sources, including tire particles, road wear particles, and brake wear [20].

In addition to the organic compounds that are incorporated into the rubber matrix — investigated further in this thesis — TRWP and brake wear contain metals and other contaminants. For instance, tire tread has been shown to have high contents of zinc (Zn), silicon (Si), and sulfur (S). ZnO and Zn stearate are added during vulcanization, while other metals such as copper (Cu), lead (Pb), nickel (Ni), chromium (Cr), and cadmium (Cd) may originate from processing agents and additives [20, 21].

Due to its heterogeneous sources, particles in road dust can vary in size. Kreider et al. found the size distribution of TRWP from road dust to lie between 4 µm and 350 µm [21]. Klöckner et al. found that TRWP content peaked in the size fraction between 20 and 50 µm. However, investigated organic tire additives peaked in smaller size fractions below 20 µm [22]. TRWP

can be transported to soils and aquatic systems through precipitation, while finer particles can become airborne and be transported through the atmosphere, where they can be deposited in remote regions [8, 9].

2.1.3. Environmental Transformation and Ecotoxicological Effects

Once released to the environment, rubber-derived compounds can leach from TRWP and form transformation products (TPs). An example is the antioxidant N-(1,3-dimethylbutyl)-N'-phenyl-p-phenylenediamine (6PPD), which reacts with ozone or other oxidants to form the highly toxic compound N-(1,3-dimethylbutyl)-N'-phenyl-p-phenylenediamine-quinone (6PPDQ) [19]. Both parent compounds and their TPs can accumulate in the environment. A recent study examining 23 rubber-derived compounds and their TPs in an urban water system found that TPs were the dominant species in surface water, raising concerns about their long-term environmental impact [23]. Similarly, Cao et al. reported the widespread occurrence of five PPD-Quinones in urban runoff, roadside soils and airborne particles, indicating widespread environmental distribution [24].

Furthermore, studies have shown that aquatic biota can ingest these compounds. In a recent study by Tian et al., 6PPDQ from stormwater runoff has been linked to coho salmon mortality on the West Coast of the United States. The compound exhibited extreme toxicity, with an LC_{50} (lethal concentration for 50 % of exposed organisms) of 0.8 µg/L [19]. Other studies have documented the ingestion of TRWP by various fish species [25], and laboratory experiments have shown that rubber-derived compounds can leach into digestive fluids of aquatic organisms, further increasing exposure risks [26]. Overall, the occurrence of TRWP and their associated chemicals represents a potential risk to aquatic organisms [27].

2.1.4. Human Exposure and Health Risks

TRWP contribute to particulate matter (PM). Recently, research focused on PM with aerodynamic diameters of 2.5 µm ($PM_{2.5}$) and 10 µm (PM_{10}), which are associated with respiratory and cardiovascular risks [28, 29]. Kole et al. estimate that 3-7 % of all $PM_{2.5}$ and 0.1-10 % of all PM_{10} may originate from tire wear [1]. A recent study on the contribution of TRWP on $PM_{2.5}$ in urban China revealed it to make up 13 % of $PM_{2.5}$ air pollution [30]. While larger particles (PM_{10}) are primarily deposited in the upper respiratory tract and swallowed, smaller respirable particles ($PM_{2.5}$) can penetrate deeper into the lungs, reaching the alveoli [31]. These finer fractions are enriched in organic pollutants and have been shown to be harmful to the respiratory system [29, 32, 33]. To distinguish between these behaviors, the term "inhale" will refer to the general intake of particles, while "respire" will specifically describe the deeper penetration of respirable particles into the lung. Recognizing these risks, the WHO set a recommended long-term exposure limit of 5 µg/m^3 for fine particulate matter exposure to

protect human health [28].

However, air quality in many cities continues to deteriorate. In February 2025, the Umweltbundesamt (German Environmental Agency) issued a warning about rising concentrations of fine particulate matter all over Germany. Due to increased energy demands, higher traffic emissions, and dry, windless weather conditions, pollutants became trapped, and air exchange was severely restricted. This led to $PM_{2.5}$ concentrations reaching up to 66 µg/m^3. Authorities advised against strenuous activities such as jogging, as increased breathing rates can result in higher intake of particulate matter [34]. This issue extends well beyond Germany or Europe. Increasing $PM_{2.5}$ pollution is a growing global concern. While the overall trend of particulate pollution is decreasing since 2010, the global average of $PM_{2.5}$ in 2022 was still at 24.2 µg/m^3, five times the limit recommended by the WHO [35]. The growing presence of TRWP in the environment raises concerns about particulate pollution. However, cities with high traffic are not the only source of exposure to particulate matter in humans. PM concentrations in indoor sports environments have been a rising concern. Salonen et al. reviewed studies on different sport environments and found PM concentrations in indoor horse riding, golf and climbing facilities to be a primary concern [36]. Indoor air quality in climbing gyms has previously been studied due to high PM concentrations originating from the use of magnesium carbonate hydroxide [37]. A recent study on indoor air quality in climbing gyms has revealed the presence of rubber-derived compounds in aerosol PM and settled dust. They reported that elevated concentrations of these compounds likely originate from the soles of climbing shoes. Climbers and employees are expected to inhale these organic compounds at significantly higher levels than from any other known sources [38].

As urbanization increases and outdoor spaces for sports and exercise become more limited, more people are expected to turn to indoor sporting facilities. Combined with worsening outdoor air quality, ensuring safe indoor air quality will become increasingly important.

Human exposure to particulate matter occurs through inhalation, ingestion, and dermal contact [39]. The inhalation of PM can cause adverse health effects to the lungs and heart [29]. The presence of rubber-derived compounds within PM can potentially exacerbate respiratory health risks, particularly since the toxicity of these rubber-derived compounds remains unclear. While much of the research on toxicity of TRWP and rubber-derived compounds has focused on aquatic organisms, studies on their effects on human respiratory systems are limited.

Existing studies on the toxicity of TRWP present conflicting findings: Some in vitro studies suggest tire debris can harm human lung cells via inhalation [18, 40] and trigger inflammatory reactions in lung epithelial and macrophage cells [40, 41]. Additionally, Li et al. found strong evidence that inhaled tire-wear microplastic particles cause lung injuries in mice [42]. In contrast, Kreider et al. reported low risk and no adverse health effects from human inhalation exposure to TRWP [21], and a rat inhalation study indicated minimal inflammation and low toxicity [43].

Rubber-derived compounds such as 6PPD, 6PPDQ, Benzotriazole (BTR), and its derivatives have been detected in human urine [14, 44], indicating potential exposure. Exposure

to BTZs, particularly 2-mercaptobenzothiazole (2SH-BTZ), in the rubber industry has also been linked to an elevated risk of bladder cancer [45]. While ingestion, leaching, and toxicity of these compounds have been demonstrated in some aquatic organisms [19, 25, 26], their bioaccessibility and potential effects in the human lung remain largely unexplored. Given the evidence of environmental presence, exposure and cellular toxicity, further research into the leaching behavior of rubber-derived compounds from TRWP in simulated human lung fluids is necessary.

Table 2.1.: List of Compounds in Tire Wear Products, their molecular formula, chemical structure, function [23, 46, 47]

Abbreviation	Molecular Formula	Chemical Structure	Function in tire wear products
Aniline	C_6H_7N		Vulcanizing additive (vulcanization accelerator)
BTZ	C_7H_5NS	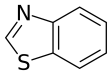	Vulcanizing additive (vulcanization accelerator)
2amino-BTZ	$C_7H_6N_2S$	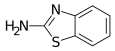	Vulcanizing additive (vulcanization accelerator)
2OH-BTZ	C_7H_5NOS	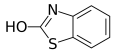	Transformation product of 2SH-BTZ
2SH-BTZ	$C_7H_5NS_2$	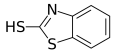	Vulcanizing additive (vulcanization accelerator)
5methyl-BTR	$C_7H_7N_3$	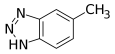	Corrosion inhibitor
DPG	$C_{13}H_{13}N_3$	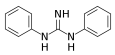	Vulcanizing additive (vulcanization accelerator)
HMMM	$C_{15}H_{30}N_6O_6$	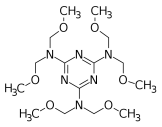	Polymer-crosslinking agent
6PPD	$C_{18}H_{24}N_2$	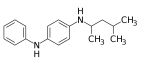	Protective additive (anti-aging agent / antiozonant)
IPPD	$C_{15}H_{18}N_2$	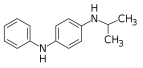	Protective additive (anti-aging agent / antiozonant)
DPPD	$C_{18}H_{16}N_2$	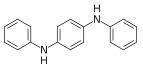	Protective additive (anti-aging agent / antiozonant)
CPPD	$C_{18}H_{22}N_2$	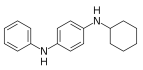	Protective additive (antiozonant / antioxidant / heat protectant)
6PPDQ	$C_{18}H_{22}N_2O_2$	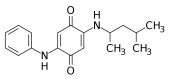	Transformation product of 6PPD
IPPDQ	$C_{15}H_{16}N_2O_2$	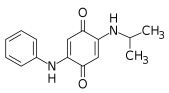	Transformation product of IPPD
DPPDQ	$C_{18}H_{14}N_2O_2$	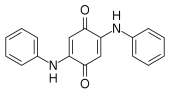	Transformation product of DPPD
CPPDQ	$C_{18}H_{20}N_2O_2$	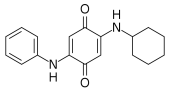	Transformation product of CPPD

2.2. Simulated Biological Fluids

The human respiratory system possesses natural defense mechanisms, such as mucociliary clearance and phagocytosis, which help to remove respired particles before they can cause potential harm. Mucociliary clearance traps particles in mucus, which is then expelled via coughing or swallowing [31, 48]. During phagocytosis immune cells, such as macrophages, engulf and then degrade pathogens [49].

However, before mucociliary clearance, rubber-derived compounds may still leach from respired particles, potentially causing toxicity to epithelial cells [18]. The thin epithelial layer may also allow translocation of leached compounds across the lung-blood barrier, resulting in systemic exposure [50]. To assess potential leaching, in vitro experiments using simulated biological fluids that mimic respiratory conditions can be conducted. One widely used solution is a modified Gamble's solution, which replicates epithelial lining fluid (the fluid covering epithelial cells). It incorporates physiologically relevant anions, cations, and organic compounds such as citrate and glycine, which substitute for proteins, along with the lung surfactant dipalmitoylphosphatidylcholine (DPPC) [51, 52]. Generally, lung surfactants are a blend of lipids and proteins that are adsorbed at the air-water interface of the alveoli cell and thereby reduce surface tension upon exhalation and inhalation [51, 53]. Given that particles may persist in the alveolar region for extended periods (months to years), long-term leaching studies are necessary to assess total organic compound release over the entire duration that a particle can remain in the lungs [48, 54].

Phagocytosis is a key immune response in the alveolar region. In this process, macrophages engulf respired particles, enclosing them in a vesicle called a phagosome. The phagosome then fuses with a lysosome, forming a phagolysosome, where enzymes break down the particle. One pathway of degradation occurs through the oxidative burst, where reactive oxygen species (ROS) are generated to aid in degradation. ROS are created through NADPH oxidase complexes and can further be converted to hydrogen peroxide (H_2O_2) by enzymes. This process is typically completed within two hours [49, 55]. Since it evolved as a defense to biological particles such as bacteria, the influence of phagocytosis on anthropogenic particles like TRWP is unclear. It can, however, be expected that particles can leach in the environment of the phagosome. A commonly used solution for in vitro experiments mimicking the environment of a phagolysosome is the phagolysosomal fluid (PSF) [56]. SLF and PSF have very different pH values, while SLF is near neutral, PSF is much more acidic.

2.3. Leaching and Mass transfer

Most rubber-derived compounds are not chemically bound to the polymer matrix which allows diffusion out of the material and facilitates leaching of these compounds into the environment [57]. While parent compounds are expected to be distributed throughout the rubber matrix, transformation products are likely located on the surface of the rubber particle. For instance,

the antioxidants added to the rubber (6PPD, N-isopropyl-N'-phenyl-p-phenylenediamine (IPPD), N,N'-diphenyl-p-phenylenediamine (DPPD), N-cyclohexyl-N'-phenyl-p-phenylenediamine (CPPD)) are expected to diffuse to the surface of the rubber and react with ozone forming a protective film around the rubber particle. The quinone product is, therefore, located at the surface [58]. Similarly, the transformation products of 2SH-BTZ, 2-hydroxybenzothiazole (2OH-BTZ) and BTZ likely form on the rubber surface due to reactions with ambient reactive oxygen species [23, 38].

The leaching of compounds from microplastics occurs through two main processes: instantaneous leaching and continuous leaching. Instantaneous leaching is time-independent and involves rapid desorption from the surface, whereas continuous leaching is time-dependent and governed by intraparticle diffusion (IPD) and aqueous boundary layer diffusion (ABLD) [59]. Understanding these mechanisms is essential for assessing the potential release of harmful compounds from TRWP in biological systems. The diffusion process inside the polymer (IPD) depends on the particle's matrix and geometry. The flux of diffusion through the aqueous boundary layer depends on the diffusion coefficient of the compound in PVC, the concentration of the compound and the thickness of the layer. The location of the compound in the rubber can, therefore, have an impact on the leaching kinetics. Compounds that are already located on the surface may leach more readily than those distributed throughout the rubber. Particle size can also influence the leaching kinetics. Smaller particles have a larger relative surface area and therefore exhibit a higher particle fluid contact. Since diffusion distances are also shorter for smaller particles, leaching kinetics of all compounds can be affected.

Henkel et al. find the governing diffusion process for phthalates from spherical PVC particles in simple aqueous systems by deriving the desorbed fraction at each time from Fick's first and second law of diffusion. They find that for IPD, the desorbed fraction depends on the particles radius and a compound- and polymer specific diffusion coefficient. For ABLD, the desorbed fraction depends on the partitioning coefficient of the compound between water and the polymer and the aqueous diffusion coefficient of the compound. Since rubber particles are generated through friction, their shape is random and often rather elongated than spherical. The approach used in Henkel et al. therefore can't be applied directly. Calculating the desorbed fraction is more challenging, since the environment of the lung is more complex and many processes occur at the same time. The exact leaching can't be quantified, since along with the release, compounds may re-sorb to other particles in the dust or transform in the lung fluid. The detected concentrations in leaching experiments can be approximately described by:

$$C_{measured} = C_{leached} - C_{resorbed} - C_{transformed} \tag{2.1}$$

The measured concentrations are therefore only a snapshot of multiple processes occurring at the same time and may underestimate the total leached amount. In a similarly complex experimental setup, two fitting models were used to describe the leaching kinetics of rubber-derived compounds in fish digestive fluids by Masset et al. [26]: A diffusion controlled model

and logarithmic model. While the diffusion-controlled model is derived from Fick's second law of extraction from a semifinite slab into solution, the logarithmic model is not directly based on a theoretical model. Nonetheless, they can be useful to provide an estimation of release of the compounds and have been previously shown to adequately fit leaching data with R^2 between 0.80 and 0.99 by Masset et al. [26]. Diffusion-controlled release can be expressed with

$$[C] = C_0 + k * t^{1/2} \tag{2.2}$$

where C is the released concentration, k the rate constant for the release [60]. The release can also be fitted with a logarithmic model expressed with

$$[C] = C_0 + k * log(t). \tag{2.3}$$

.

Masset et al. find in their leaching studies of rubber-derived compounds from cryogenically milled tire tread into simulated fish intestinal and gastric fluids, that most compounds — except polycyclic aromatic hydrocarbons (PAHs) —were solubilized rapidly within 3 hours in gastric fluid and 24 hours in intestinal fluid. Higher bioaccessible fractions were observed for more polar compounds such as aniline, BTZ and DPG than for more hydrophobic PAHs. Overall, the solubilization potential was similar in all fluids for polar compounds, indicating little influence of pH and enzymes to the leaching behavior [26].

An important parameter in leaching experiments is the solid-to-liquid ratio. In bioaccessibility studies of metal(loids), ratios typically range between 1:20 and 1:50000 with many studies using ratios below 1:100 [51]. A realistic respiration scenario in a climbing gym would result in a ratio of 1:2000, based on respirable PM concentrations measured in climbing gyms (~10.5 mg in a three hour climbing session [38]) divided by the total lung fluid volume (20 mL [61]). However, this ratio is relatively low compared to ratios used in previous leaching studies with rubber-derived compounds, such as 1:10 used by Masset et al. [26], and compounds may not be detectable at this level. Since particles are unlikely to interact with the whole lung fluid volume, it can be assumed that higher ratios (1:1 or 1:10) may offer a more realistic representation of the exposure, to the best of our knowledge there are no studies that have explicitly investigated this. For PSF, higher solid-to-liquid ratios (1:1) can even be considered, since the phagosome encapsulates much less fluid.

Knowing the physico-chemical properties of the compounds can help to better understand the leaching kinetics and detected concentrations. For instance, the octanol/water partition coefficient $\log K_{OW}$ indicates a compound's tendency to partition between aqueous and organic phases. It can provide an insight into how quickly rubber-derived compounds may leach into biological fluids. In general, hydrophilic compounds are expected to leach faster and more easily than hydrophobic ones [26]. Specifically, diffusion through the ABLD can be expected to be slower for hydrophobic compounds.

For the purpose of this study, hydrophilic compounds were classified with a $\log K_{OW}$ below 3 and hydrophobic compounds above 3. However, since many rubber-derived compounds are ionizable, the $\log K_{OW}$ is not always suitable for describing partitioning. Instead, the partition coefficient logD can be used, which reflects a compound's pH-dependent partitioning.

The value of logD is influenced by the compound's ionization state, which is given by its pK_a. The pK_a is the logarithm of the acid dissociation constant, indicating the pH at which the compound is 50 % ionized. The lower the value of LogD, the more hydrophilic the compound, a higher value indicates a compounds tendency to be lipophilic, preferring organic phases over water. Due to its pH dependent variation, this value can better describe the compound's behavior in a biological environment [62]. In the present study, the simulated lung fluids have very different pH levels: SLF has a slightly alkaline pH of 8.4, while PSF is at pH 4.5.

The pK_a indicates the pH at which the compound is protonated (below the pK_a) or deprotonated (above the pK_a). If a compound is acidic, it will be negatively charged above the pK_a, and if it is basic, it will be positively charged below it. The charge of a compound significantly influences its sorption affinity. For example, at lower pH, basic organic compounds are positively charged and exist primarily in their cationic form. This allows them to adsorb more easily to negatively charged particles and mineral surfaces through electrostatic interactions. LogD values for acids and bases were calculated with [62]:

$$logD_{acids} = logK_{OW} + log\left(\frac{1}{1+10^{pH-pK_a}}\right) \tag{2.4}$$

$$logD_{bases} = logK_{OW} + log\left(\frac{1}{1+10^{pK_a-pH}}\right) \tag{2.5}$$

and are shown in Table 2.2.

The stability of a compound in solution is a critical factor in interpreting release kinetics. For instance, if the measured concentration of an unstable compound remains constant in the leachate, this can indicate a continuous release of the compound, but due to its instability no increase in concentration is observed. Many rubber-derived compounds are known to undergo oxidative transformations under ROS exposure. For example, 6PPD is known to react with ozone to form 6PPDQ [70], and similar reactivity can be expected for other PPDs. Additionally, the transformation products 2OH-BTZ and BTZ, derived from 2SH-BTZ, also result from oxidation, a process previously shown to be induced by ozone [71].

Since ROS are generated within the phagosome, it is likely that these compounds will undergo transformation in such environments. To simulate this oxidative condition, H_2O_2 is added to PSF. Consequently, the stability of many compounds in PSF containing H_2O_2 is expected to be significantly reduced. The compounds are expected to show different release kinetics in different fluids. Some compounds are highly unstable in aqueous solution, such as 6PPD with a half-life of 8 hours [72], whereas the quinone derivative is more stable with a

Table 2.2.: Physicochemical properties of the studied compounds, including pKa and partition coefficients (log D) at different pH values.

Compound	$\log K_{OW}$	pK_a	$\log D_{4.55}$	$\log D_{8.4}$
Aniline	0.9 [63]	4.6 [64]	0.57	0.90
BTZ	2.17 [65]	2.28*	2.17	2.17
2amino-BTZ	2 [65]	3.58*	1.96	2.00
2OH-BTZ	2.35 [65]	8.9 [66]	2.35	2.23
2SH-BTZ	1.85 [65]	7.1 [66]	0.84	-2.97
5methyl-BTR	1.13 [67]	8.5 [66]	1.13	0.88
DPG	2.42 [68]	9.74 [69]	-2.77	1.06
HMMM	1 [63]	3.6 [69]	0.95	1.00
6PPD	4.47 [24]	6.46 [24]	2.55	4.47
IPPD	3.28 [24]	6.42 [24]	1.40	3.28
DPPD	4.93 [24]	2.42 [24]	4.93	4.93
CPPD	4.64 [24]	6.42 [24]	2.76	4.64
6PPDQ	3.98 [24]	0.61 [24]	3.98	3.98
IPPDQ	2.58 [24]	0.87 [24]	2.58	2.58
DPPDQ	3.46 [24]	0.47 [24]	3.46	3.46
CPPDQ	3.94 [24]	0.62 [24]	3.94	3.94

* calculated by Chemicalize Software

half-life of 33 hours (at 23°C) in dechlorinated tap water [73]. The biological half-life of DPG in rats is reported to be about 9.6 hours [74] and the half-life if 2SH-BTZ in rats was less than 8 hours [75].

Aims and Hypotheses

To address the gaps in our understanding of the leaching of rubber-derived compounds in the respiratory system, in vitro leaching experiments were conducted using respirable road and climbing hall dust in simulated lung fluids. This thesis investigates the release of rubber-derived compounds from these two dust samples in simulated epithelial lung fluid (SLF) and phagolysosomal fluid (PSF).

The primary aim of the study is to compare the release kinetics of rubber-derived compounds in SLF and PSF from respirable road and climbing hall dust, and to evaluate whether this release occurs rapidly or continuously over the leaching time frame. Compounds with lower $\log K_{OW}$ are expected to leach in higher concentrations. These aims are addressed through leaching experiments conducted over the course of a week in SLF and over two hours in PSF. To quantify release, bioaccessible fractions are calculated by comparing leached concentrations to the total amount extractable from the dust. To mimic the more oxidative environment of the phagolysosome, leaching studies in PSF are conducted with and without the addition of H_2O_2. Many rubber-derived compounds have been shown to be highly unstable. To account for compound instability, additional stability tests of the investigated rubber-derived compounds

are conducted in SLF and PSF, with and without H_2O_2.

Based on prior findings and theoretical considerations, the following hypotheses are proposed:

1. Parent compounds, which are likely distributed throughout the rubber, are expected to leach gradually over the course of a week. In contrast, transformation products, which likely form on the rubber's surface, are expected to be released rapidly in SLF.

2. Since parent compounds, such as 2SH-BTZ and PPDs, are known to transform under oxidative conditions, the oxidative environment in PSF—due to the addition of H_2O_2—is expected to reduce the stability of those parent compounds, promote their degradation, and consequently lead to increased levels of their transformation products (2OH-BTZ, BTZ and quinone derivatives) in the leachate.

3. Materials and Methods

3.1. Chemicals and Materials

For the preparation of lung fluids, NaCl, NH_4Cl, dipalmitoylphosphatidylcholine (DPPC), potassium hydrogen phthalate, Na_3 citrate·$2H_2O$, Na_2SO_4·$10H_2O$, alkylbenzyldimethylammonium chloride (ABDC), potassium hydroxide solution, and formic acid (for UPLC analysis) were purchased from Merck. $CaCl_2$·$2H_2O$, Na_2HPO_4 and Glycine were purchased from Sigmal-Aldrich. Na_2SO_4 from Honeywell, hydrogen peroxide from Acros, $NaHCO_3$ from Thermo Scientific, and $MgCl_2$·$6H_2O$ from VWR. LC-MS grade acetonitrile was purchased from Fisher Scientific and Ultrapure water was produced using a PURELAB Chorus system (0.071 µS/cm, Elga Veolia). 16 rubber-derived compounds were used as stocks for calibration standards. BTZ, 2OH-BTZ, 2SH-BTZ, 2amino-BTZ,DPG, aniline, 6PPD, 5methyl-BTR were purchased from Sigma-Aldrich, 6PPDQ, IPPD, IPPDQ, DPPD, DPPDQ, CPPD, CPPDQ, and d5-6PPDQ were purchased from HPC Standards. HMMM was purchased from TCI Europe and d4-BTZ from LGC Standards.

3.2. Sample Collection and Preparation

Road dust samples were collected at Althangrund/Josef-Holaubek-Platz, Vienna (48.233209 N, 16.358449 E). A location with frequent pedestrian crossings and braking was chosen. Samples were collected following several days of dry weather (03/04/2024 and 11/05/2024) with a spatula and brush and stored in a 50 mL centrifuge tube until further preparation. Climbing hall dust was collected from the air filter of a climbing gym and also stored in a 50 mL centrifuge tube.

Particulate matter samples collected from the climbing hall and the road were size separated using the Next Generation Pharmaceutical Impactor (NGI) following a dust size separation protocol developed by Wimmer and Sherman. The NGI, in combination with a low capacity LCP6 vacuum pump set to a constant flow rate of 60 L/min ± 2 L/min, enabled precise aerodynamic particle separation. A cyclohaler mouthpiece facilitated controlled sample delivery.

The NGI consists of eight trays, each targeting specific particle aerodynamic diameters. Based on D50 value (aerodynamic diameter of a particle at which 50 % of the particles are smaller and 50 % are larger), tray 1 collects the inhalable fraction, while trays 2 to 8 capture the respirable fraction (D50 ≤4.46 µm) (see Fig. 3.1).

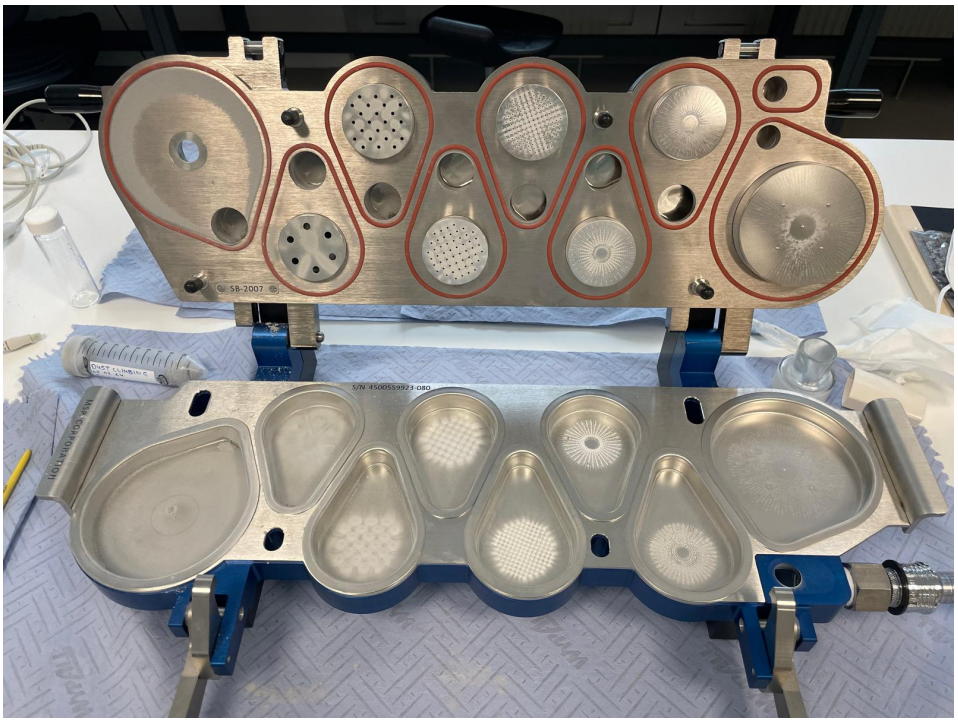

Figure 3.1.: Next Generation Pharmaceutical Impactor for Dust Size Separation. Trays 1-8 from left to right.

Before each run, all equipment was cleaned, dried, and weighed. The cyclohaler was filled with the dust sample and connected to the NGI, with the pump running for 30 seconds per cycle. This process was repeated until flow rate deviations indicated clogging, after which trays were weighed and the collected dust from trays 2-8 combined and recorded. Between samples, cleaning prevented cross-contamination.

The D50 values for NGI trays depend on volumetric flow rate and were calculated using Eq. (3.1), ensuring consistent aerosol size separation. Fig. 4.3 presents the size distribution of road and climbing hall samples across multiple runs, demonstrating reproducibility. One run was defined as completing the protocol until clogging occurred.

$$D_{50,Q} = D_{50,60\,\mathrm{L/min}} * \left(\frac{60}{Q}\right)^{X} \tag{3.1}$$

where Q is the volumetric flow rate, X and $D_{50,60\,\mathrm{L/min}}$ are given in Table A3.

3.3. Dust Extraction

Dust samples were extracted with Accelerated Solvent Extraction (ASE, Thermo-Fisher). Before filling in the dust, the extraction was performed once on the empty cells. All samples were extracted in triplicate. After adding a GF/F filter and filling the ASE cells with glass beads, dust was weighed in at 50 ± 0.01 mg. All samples were spiked with 20 µL of d4-benzothiazole (d4-BTZ) and d5-6PPD-quinone (d5-6PPDQ) each at a concentration of 10 µg/mL (for a final

concentration of 100 µg/L). The extraction included three static cycles of 5 minutes with 100 % acetonitrile (LCMS grade) as solvent under 80 ° C. Two method blanks were prepared in the same way as the samples. After extraction, samples were stored in the fridge (storage for 14 days) until they were evaporated with nitrogen blowdown at room temperature. Samples were concentrated to 0.5 mL, then reconstituted to 2 mL with acetonitrile with a pasteur pipette and vortexed and filtered through 0.22 µm nylon filters using syringe filtration before analysis.

3.4. Preparation of Lung fluids

The simulated epithelial lung fluid (SLF) was designed to simulate epithelial lung lining fluid. The SLF formulation used here was a modified Gamble's solution [76], optimized to analyze toxic elements from volcanic ash [52]. The modifications include the addition of representative anions and functional groups such as glycine and the addition of the lung surfactant dipalmitoylphosphatidylcholine (DPPC). Exact composition is detailed in Table A1.

To prepare the SLF, stocks were prepared in ultrapure water and underwent sonication for 15 minutes and were subsequently heated at 70°C for 10 minutes. Finally, the prepared solutions were transferred to glass vials and Schott bottles for storage. All individual stock volumes were combined in a Schott Bottle. Ultrapure water was then added to bring the total volume to 250 mL, constituting the final SLF solution. The pH of the SLF was between 8.4 and 8.5. The SLF was stored at 4°C.

A phagolysosomal fluid (PSF) was prepared similarly to the SLF, following a protocol from Stefaniak et al. [56]. To imitate the oxidative burst, one variant of PSF was prepared with hydrogen peroxide (H_2O_2) and one without. Stocks were prepared in ultrapure water, sonicated for 15 minutes and heated for 10 minutes at 70°C. Stocks were stored at 4°C in glass vials and Schott bottles. For the PSF, stocks were added for required concentrations detailed in Table A2 and filled to appropriate volume with ultrapure water. To avoid degradation before the experiment, the hydrogen peroxide was only added before starting the leaching experiment. Before, both solutions were adjusted to a pH of 4.55 with 1 mol/L potassium hydroxide solution.

3.5. Leaching Experiment

Leaching experiments were conducted using SLF with solid-to-liquid ratios of 1:200 and 1:20 and for PSF a 1:20 ratio was used. The 1:20 ratio was selected as the highest feasible ratio within the experimental setup. Preliminary tests at different ratios (1:2000, 1:1000 and 1:200) showed only sporadic detections of leached rubber-derived compounds in the 1:2000 setup, but consistently quantifiable results at 1:200 (see Table A8).

Since preliminary experiments showed difficulties in surrogate standard recovery, the 1:200 SLF leaching experiment was conducted with n=5 replicates. After successfully recovering the surrogate standard for all replicates, the experiments after (all other leaching and stability

experiments) included n=3 replicates. For the 1:200 ratio, dust samples (5 replicates, each 10 mg) were weighed into Eppendorf tubes. Subsequently, 2 mL of SLF was added to each tube. For the 1:20 ratio, used in SLF and PSF experiments, 75 mg of dust was weighed in and 1.5 mL of fluid was added to the Eppendorf tube. Method blanks, containing only fluids, were prepared following the same procedure.

All tubes were vortexed and then placed in an Eppendorf ThermoMixer set at 37°C, with agitation at 1500 rpm, in the dark. This agitation allowed thorough suspension and mixing of the particles in the fluid. For SLF, the experiment was conducted over the course of a week. Samples were placed in the ThermoMixer and taken out at specific time points and extracted (sacrifical sampling). Extraction points were after 10 minutes, 1 hour, 3 hours, 8 hours, 24 hours, 48 hours, 72 hours and 168 hours. For PSF, the total experiment lasted 2 hours, with extraction times after 10 minutes, 30 minutes, 1 hour and 2 hours. At the respective extraction time point, samples were centrifuged at 20°C and 20000 rcf for 20 minutes, followed by a liquid-liquid extraction.

For the 1:200 ratio, 1.5 mL of the supernatant was pipetted into a new glass vial, and an equal volume of acetonitrile (1.5 mL) was added. Each sample was spiked with 25 µL of a mixed surrogate standard solution containing d4-BTZ and d5-6PPDQ in acetonitrile, each at a concentration of 10 µg/mL, achieving a final concentration of 100 µg/L of surrogate standard in the sample. To achieve phase separation, 100 mg of salt was added to each vial, followed by vortexing. For the 1:20 ratio, only 1 mL of supernatant was pipetted into a glass vial with 1 mL of acetonitrile. Samples were then spiked with 20 µL of a mixed surrogate standard solution for a final concentration of 100 µg/L. 66.6 mg of salt was added and samples were vortexed.

For both ratios, the mixture was left to settle for one minute, then the top organic layer was extracted using a Pasteur pipette into a new glass vial. A second round of extraction was performed with an additional 1 mL of acetonitrile, followed by vortexing, allowing separation, and extracting the top layer. The combined extract was subsequently vortexed and filtered through 0.22 µm nylon filters into LCMS vials for analysis.

To relate leaching kinetics to compound stability in the lung fluids, 2 mL of SLF or PSF were added to Eppendorf tubes and spiked with a rubber additive mixture (400 ng/mL). Samples underwent the same procedure with thermo mixer and liquid-liquid extraction at the same time points as in the leaching experiment and consequently measured with LC-MS/MS.

3.6. UPLC-MS/MS

All samples were analyzed with ultra-performance liquid chromatography coupled to triple quadrupole mass spectrometry (Agilent 1290 Infinity II - Agilent 6470) utilizing a T3 C18 column (Acquity HSS T3, 1.8 µm, Waters) in positive ionization mode with a capillary voltage set at 2500 V. This analysis employed multiple reaction monitoring (MRM). The liquid chromatography operated at a flow rate of 0.6 mL/min with the column maintained at a temperature

of 40 °C, and an injection volume of 5 µL. The multisampler was kept at a temperature of 10°C. The mobile phase consisted of ultrapure water (Phase A) and acetonitrile (Phase B), both containing 0.1 % formic acid. The eluent gradient was kept at 95 % Phase A for one minute, then Phase B was increased to 95 % over 9 minutes while Phase A decreased to 5 %. This was held constant for two minutes until Phase A was increased again for one minute to 95 %. Electrospray Ionization occurred at a temperature of 240°C and a gas flow of 5 L/min. The nebulizer was set to 30 psi, sheath gas to 25 °C and 11 L/min. 16 compounds were investigated (see Table 2.1). See appendix for method report with transitions from precursor and product Ion and quantifiers (Table A7) and LOQ of the compounds in all experiments (Table A5).

3.7. Scanning Electron Microscopy

For assessment of the morphology of the two dust samples, Scanning Electron Microscopy (SEM) was performed. Samples were prepared by placing a double sided carbon tape on the SEM stub and coating it with a layer of dust material. Subsequently, samples were sputtered with carbon with the LEICA EM SCD 500 and measured with the TESCAN Vega 4 GMU Scanning Electron microscope. The acceleration energy amounted to 10 keV, the beam current was at 10 pA and the working distance was set to approximately 10 mm.

3.8. Data analysis

Quantification of all data measured with UPLC-MS/MS was performed with Agilent MassHunter (QQQ) quantitative analysis software. Data was further processed with R version 4.3.1.. For outlier detection for samples with 5 replicates the inter-quartile method for outlier detection was used. For samples with triplicates, a manual outlier detection was chosen by excluding data points that were out of range of the other two replicates.

3.9. QA/QC

For the dust extraction, thirteen calibration standards were prepared by diluting rubber additive mixed stocks in acetonitrile to concentrations between 0.1 µg/L and 750 µg/L. Recovery was evaluated by spiking all compounds directly into the ASE cell, followed by extraction using the standard protocol (see Table A4). Method blanks in dust extractions detected BTZ exclusively. To address this, the mean concentration of BTZ measured in blanks was subtracted from the respective sample concentrations. No other compounds were detected in method blanks.

For the leaching experiments, seventeen matrix-matched calibration standards ranging from 0.01 µg/L to 1000 µg/L were prepared in the same matrix as the samples. Rubber-derived compounds dissolved in acetonitrile and spiked into SLF/PSF followed by liquid-liquid extraction

(R^2 for calibration curves can be found in Table A6). Due to this matched-matrix calibration, the recovery and matrix effects of compounds were inherently accounted for during the preparation of the calibration standards.

Instrument blanks consisting of solvent and spiked with surrogate standard (d5-6PPDQ and d4-BTZ) were used as reference of possible contamination occurring through the measurement. In SLF stability and leaching occasionally showed DPG contamination in the instrument blanks. Two blanks in the SLF 1:20 with a mean of 0.64 ± 0.06 µg/L and three blanks in SLF stability with a mean of 3.77 ± 0.04 µg/L were detected. The Limit of Quantification (LOQ) was adjusted for DPG using:

$$LOQ = mean(blanks) + 3 * Std_{dev}(blanks). \tag{3.2}$$

For all other compounds, the LOQ was determined from the lowest linear point in the calibration curve.

Method blanks were prepared identically to samples with one method blank for each extraction time point. In the SLF experiment at a ratio of 1:200, the method blanks also served as control samples placed in the thermo mixer with the samples to account for contamination from the eppendorfs or fluids themselves and extracted at corresponding time points. Only DPG was detected in these control samples and was subtracted to account for the contamination. As no additional rubber-derived compounds were detected, it was concluded that no contamination was introduced during the leaching experiment. Thus, for all further experiments, method blanks were not placed in the thermo mixer but were simply prepared at each extraction time point and extracted along with the sample to account for any contamination during sample extraction. At the ratio of 1:20, both DPG (between 0.40 and 0.42 µg/L) and 2SH-BTZ (between 0.53 and 1.05 µg/L) were detected in method blanks and subtracted accordingly. In SLF stability experiments, DPG was measured in all method blanks (between 3.72 and 3.76 µg/L) and subtracted. Additionally, 5methyl-BTR (8.01 µg/L), CPPD (1.13 µg/L), BTZ (0.98 µg/L), 6PPDQ (1.30 µg/L) and 2SH-BTZ (1.80 µg/L) were detected each in one method blank and subtracted accordingly.

In Leaching and Stability experiments for PSF, multiple compounds were detected in method blanks and subtracted. DPG showed concentrations between 0.81 µg/L and 0.98 µg/L in all blanks (with and without H_2O_2), BTZ was detected in one blank without H_2O_2 at 3.63 µg/L and DPPDQ was found in one control at 4.61 µg/L. The blanks without H_2O_2 showed high 2SH-BTZ contamination mostly between 5.19 µg/L and 5.90 µg/L. The one hour method blank detected concentrations at 50.12 µg/L, leading to zeroing concentrations at specific time points for PSF without H_2O_2 in the Leaching. Blanks in the stability experiments also detected DPG in all controls between 1.21 µg/L and 1.65 µg/L. 6PPD was detected in the control samples without H_2O_2 at concentrations between 0.06 µg/L and 0.07 µg/L. The one and two hour method blank with H_2O_2 showed a contamination of 2SH-BTZ of 859.68 µg/L leading to zeroing concentrations for the samples. One blank in the fluid with H_2O_2 showed concentration of 7.44 µg/L

for 5methyl-BTR.

All samples were spiked with surrogate standards of d4-benzothiazole (d4-BTZ) and d5-6PPD-quinone (d5-6PPDQ) to monitor recovery and instrument performance. Detected concentrations were surrogate standard corrected. These standards were spiked in the extraction process before adding NaCl. In PSF samples with H_2O_2, surrogate standards degraded, requiring analysis without them. Glassware was cleaned using a dishwasher, followed by sequential rinses with ultrapure water, acetonitrile, and isopropanol, and oven-drying prior to use.

3.10. Bioaccessible fraction

To quantify the extent of leaching for each compound and compare different compounds with each other, a comparison of the concentrations observed in the leaching experiment with the total concentrations of the compound available from dust extraction is necessary. This comparison yields the bioaccessible fraction, which is the ratio of leached to extracted compounds.

Bioaccessible fractions were calculated with the leached concentration at the end of each experiment: for SLF, the 168-hour time point was used, and for PSF, the 2-hour time point was selected. For unstable compounds, these time points may not accurately reflect the total released fraction and could result in underestimations. Despite this limitation, the method enables relative comparisons between different compounds. The bioaccessible fraction was calculated by first converting the mean leached concentrations from µg/L to ng/mg. This was achieved by multiplying the leached concentration with the amount of lung fluid used (2 mL for the 1:200 ratio and 1.5 mL for the 1:20 ratio), and then dividing by the amount of dust used (10 mg for the 1:200 ratio and 75 mg for the 1:20 ratio). Once the concentration was converted to ng/mg, this value was divided by the mean concentration of dust extracted and multiplied by 100 to express the result as a percentage (Eq. (3.3)) Additionally, the standard deviation for the bioaccessible fraction was calculated using the principles of error propagation for division (Eq. (A1))

$$Bioaccessible = \frac{C_{Leached}}{C_{Extracted}} * 100 \tag{3.3}$$

4. Results and Discussion

4.1. Finer Particle Sizes in Climbing Hall Dust Compared to Road Dust

Road and climbing hall dust originate from different environments and collection methods, leading to distinct physical characteristics. Climbing hall dust was collected from air filters, where airborne particles are trapped, leading to finer and more homogeneous particle size distribution. In contrast, road dust was obtained from the road surface, containing particles of varying sizes and compositions from multiple sources.

Scanning Electron Microscopy (SEM) analysis revealed that the road dust sample still contained large particles (Fig. 4.1a), although the fractionation process should have excluded particles larger than those with a D50 of 4.42 µm in the respirable fraction. Rubber particles generated through friction (either the tire with the road or the climbing shoe with a foot hold) are often elongated in shape and encrusted with minerals originating from pavement or other environmental sources [77]. Potential rubber particles within the desired size range were observed in the sample (Fig. 4.1b), but the presence of larger particles indicates that the fractionation was unsuccessful and road dust cannot be considered respirable. The presence of these larger particles may influence the leaching behavior and resulting concentrations.

Since the same size separation method was applied to both dust types, the heterogeneity of road dust likely contributed to the unsuccessful fractionation. The NGI instrument was prone to clogging, particularly during road dust analysis. This necessitated increasing the vacuum pump output to maintain the desired flow rate, potentially compromising the effectiveness of the separation. To improve future fractionation processes, pre-sieving of the road dust to exclude particles larger than 100 µm could reduce the risk of clogging and improve sample homogeneity. Additionally, frequent cleaning of the NGI before clogging occurs can possibly enhance the accuracy of the fractionation. Alternative sampling techniques, such as the use of hand-held vacuum cleaners followed by sieving — as reported in previous studies [78], could further improve sample homogeneity before NGI fractionation.

In contrast, the fractionation of climbing hall dust was successful. SEM images (Fig. 4.2a) showed small particles, some of which were stacked on top of each other, but no larger particles were observed. Potential rubber structures within the desired size range were also observed, as shown in Fig. 4.2b.

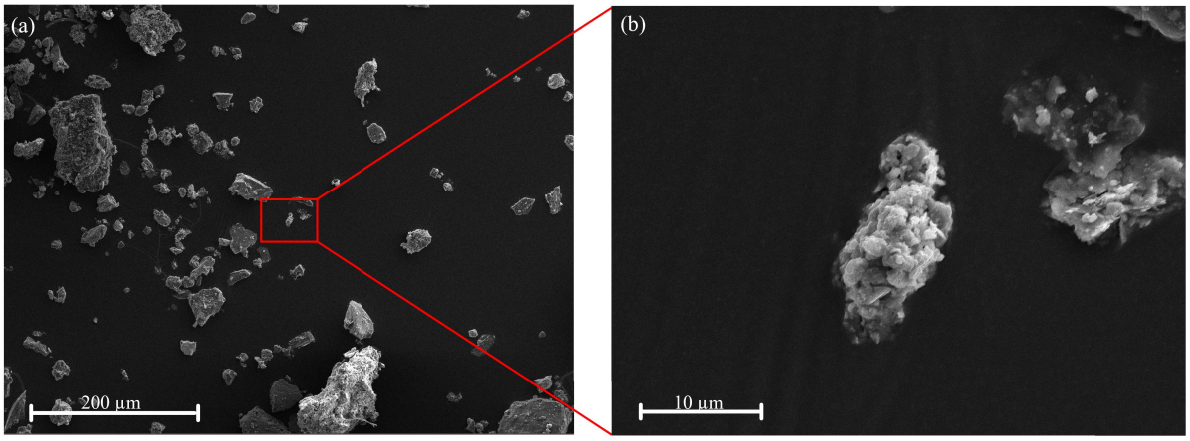

Figure 4.1.: Scanning Electron Microscopy (SEM) of road dust: (a) overview and (b) zoom on a possible rubber particle. Working Distance: 9.96 mm.

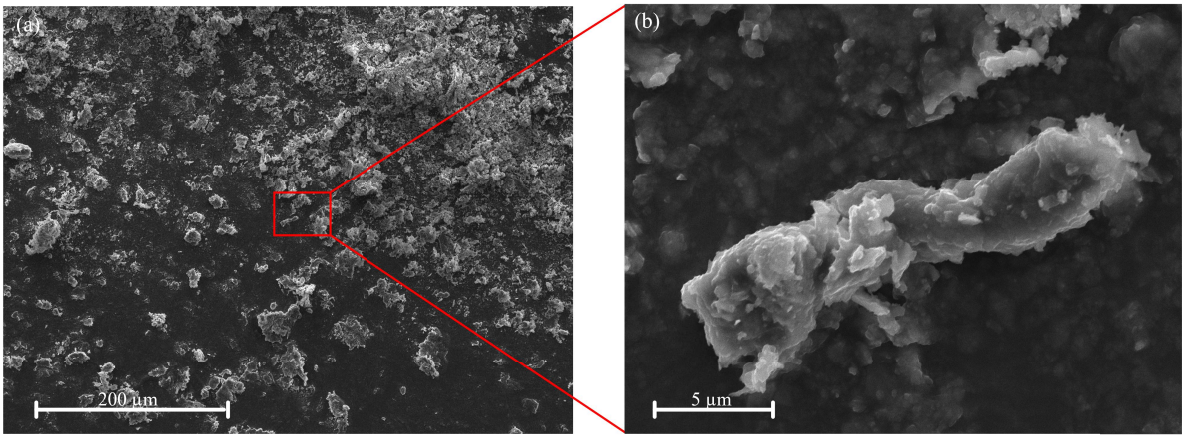

10

Figure 4.2.: Scanning Electron Microscopy (SEM) of climbing hall dust: (a) overview and (b) zoom on a possible rubber particle. Working Distance: 9.98 mm.

Fig. 4.3 illustrates the particle size distribution of the respirable fraction from the NGI . Road dust exhibited a greater proportion of larger-diameter particles (Fig. 4.3a), while climbing hall dust displayed a higher mass fraction in the smaller size range (Fig. 4.3b). This observation supports the hypothesis that road dust consists of slightly larger particles.

Given these differences, a direct comparison between road and climbing hall dust is not appropriate. Therefore, subsequent analysis of leaching kinetics in the three simulated lung fluids will focus on comparison within one dust sample (road or climbing hall dust), particularly with a focus on the respirable fraction of climbing hall dust.

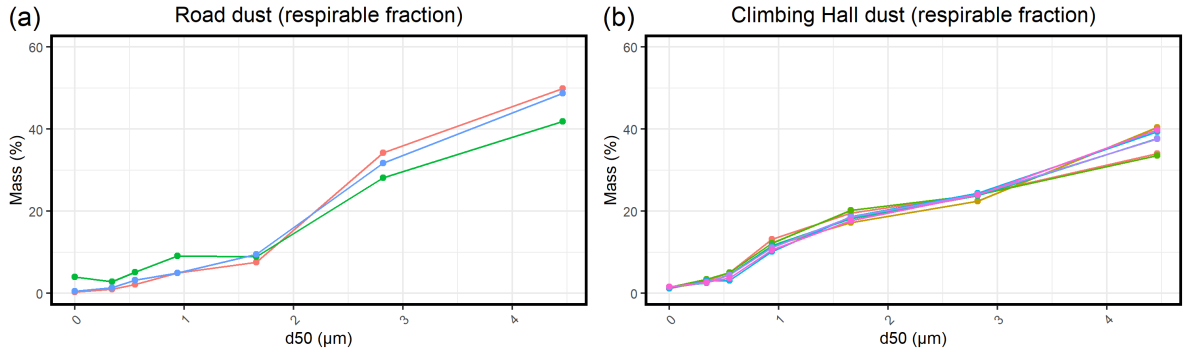

Figure 4.3.: Particle size distribution of the respirable fraction of (a) road dust and (b) climbing hall dust. Colors indicate different runs in the NGI.

4.2. Presence of Rubber-derived Compounds in Dust Samples

To determine the composition of the dust samples, a targeted analysis of 16 rubber-derived compounds was performed using Accelerated Solvent Extraction (ASE). The names, structures and functions of these compounds are presented in Table 2.1. Eleven of the 16 compounds were detected. Among these, 6PPD, 6PPDQ, BTZ, DPG, HMMM and IPPD were consistently present in both dust types (see Fig. 4.4).

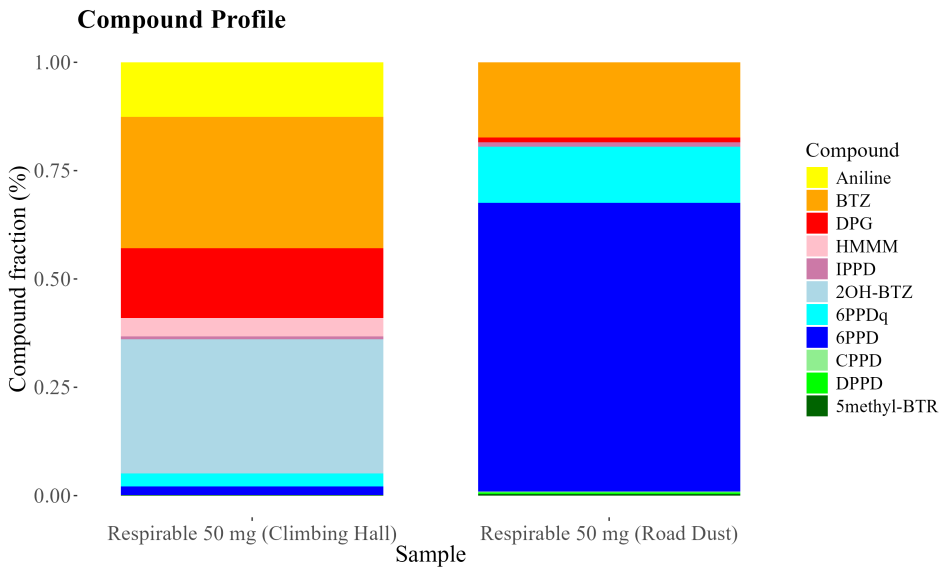

Figure 4.4.: Compound Profile from Dust Extraction.

In road dust, nine compounds were detected. The highest concentration was found for 6PPD (0.68 to 2.81 ng/mg), followed by its transformation product 6PPDQ (0.12 to 0.81 ng/mg) and BTZ (0.16 to 1.13 ng/mg). Lower levels of IPPD, DPG, HMMM, and DPPD were also observed. These findings align with previous studies on road dust and tire and road wear particles (TRWP), which reported 6PPD and 6PPDQ as the most abundant PPDs, along with elevated levels of BTZ. While the presence of PPDs is a clear indicator of rubber in the dust, as they are predominantly used in the tire-rubber industry, BTZs are also common in various industrial contexts [78].

Klöckner et al. sampled tunnel dust and found 6PPDQ to range from 220 to 290 ng/mg, followed by 6PPD between 1.5 and 1.9 ng/mg. These higher values can be attributed to tunnel environments, which experience higher TRWP accumulation due to the less diverse particle sources and the absence of precipitation [22]. Huang et al. reported 6PPD concentrations between 4.1 and 238 ng/mg and 6PPDQ between 3.0 and 88.1 ng/mg in road dust sampled from 20 sites across a Chinese megacity [79]. Deng et al. found in their study on road dust a median of 2.65 ng/mg for BTZ, 0.80 ng/mg for 6PPD, and 0.27 ng/mg for 6PPDQ [78]. These values align better with our measured concentrations, indicating a better comparison with dust from the open road. This suggests that the sampled dust is representative of road dust respired by people and, due to smaller concentrations than in the literature, might even be an underestimation of exposure levels.

However, road dust is highly heterogeneous and while Deng et al. sampled at 10 different and Huang et al. at 20 different sampling points, road dust in this study was collected from a single location. Broader sampling would be necessary for more comprehensive comparisons.

In climbing hall dust, eight compounds were detected, aligning with recent findings by Sherman et al. [38], who reported nine rubber-derived compounds. In this study, concentrations of 2OH-BTZ ranged between 1.71 and 2.97 ng/mg, followed by BTZ between 1.26

and 2.89 ng/mg. DPG, aniline, HMMM, and the PPDs were found in lower concentrations. Compared to Sherman et al., concentrations in this study were slightly lower but still within a comparable range.

Their reported 2OH-BTZ concentration (1.42 to 3.11 ng/mg) and BTZ (2.74 and 13.89 ng/mg) and higher aniline and DPG levels may be explained by their sampling method (aerosol PM collected in liquid), in contrast to our filter dust collection.

The absence of 2SH-BTZ, a common rubber-derived compound in climbing shoes, is likely due to atmospheric transformation into 2OH-BTZ and BTZ once rubber particles are formed and become airborne in the climbing gym. Additionally, low recovery rates for 2SH-BTZ in the extraction method may have led to underestimations (see Table A4).

In general, climbing hall dust exhibited slightly higher concentrations of BTZs, whereas road dust contained elevated levels of PPDs, as illustrated in Fig. 4.4. This can likely be attributed to the differences in rubber in the two samples. Tires are exposed to much more ozone, necessitating higher concentrations of PPDs than for the rubber in climbing shoes. Previous research has shown that concentrations of organic rubber-derived compounds increase from coarser to finer fractions [22]. Climbing hall dust (size: D50 $\leq$4.42 µm) is fully within the respirable range, while road dust includes much coarser particles. Thus, higher concentrations of rubber-derived compounds in climbing hall dust would be expected.

However, leachate concentrations were often higher for road dust. One explanation for this may be that the dust morphology affected extraction efficiency. Despite identical extraction procedures, road dust's larger particles may have decreased extraction efficiency, rendering the method less effective compared to the fine, homogeneous particles in climbing hall dust.

4.3. Bioaccessible Fractions for the different fluids and solid-to-liquid ratios

In order to compare leached concentrations in the different fluids, the bioaccessible fraction was calculated from the total leached amount divided by the total extracted amount. For both SLF and PSF the final time point of measurement were used for the total leached amount, which was 168 hours for SLF experiments and the 2 hour time point for PSF experiments. Bioaccessible fraction could only be identified for compounds above the limit of quantification in both extraction and leaching experiments. This was the case for aniline, BTZ, DPG, HMMM, IPPD, 2OH-BTZ, 5methyl-BTR, 6PPD and 6PPDQ.

In road dust, extremely high fractions were observed for some compounds, particularly in the 1:200 solid-to-liquid ratio. For instance, only 0.04 ng/mg of DPG was extracted, while 4.32 ng/mg were detected in the 1:200 leachate, resulting in a bioaccessible fraction exceeding 10,000 % (See appendix: Fig. B1).

Other road dust samples also showed elevated DPG fractions (1000-2000 % in SLF and PSF at 1:20 ratio). In contrast, climbing hall dust yielded DPG extraction concentrations of

0.77 ng/mg, with SLF bioaccessible fractions ranging between 100-300 % and only between 45 % to 48 % in PSF (Fig. 4.5). For road dust, bioaccessible fractions were also very high for 5methyl-BTR (all above 100 %). The extracted amount for this compound was very low, likely leading to an overestimation of the bioaccessible fraction. In general, due to the difference in particle size, it can be expected that road dust extraction was much slower and possibly less successful than that of the respirable climbing hall dust. This could be an explanation for the bioaccessible fractions of >100 % in road dust.

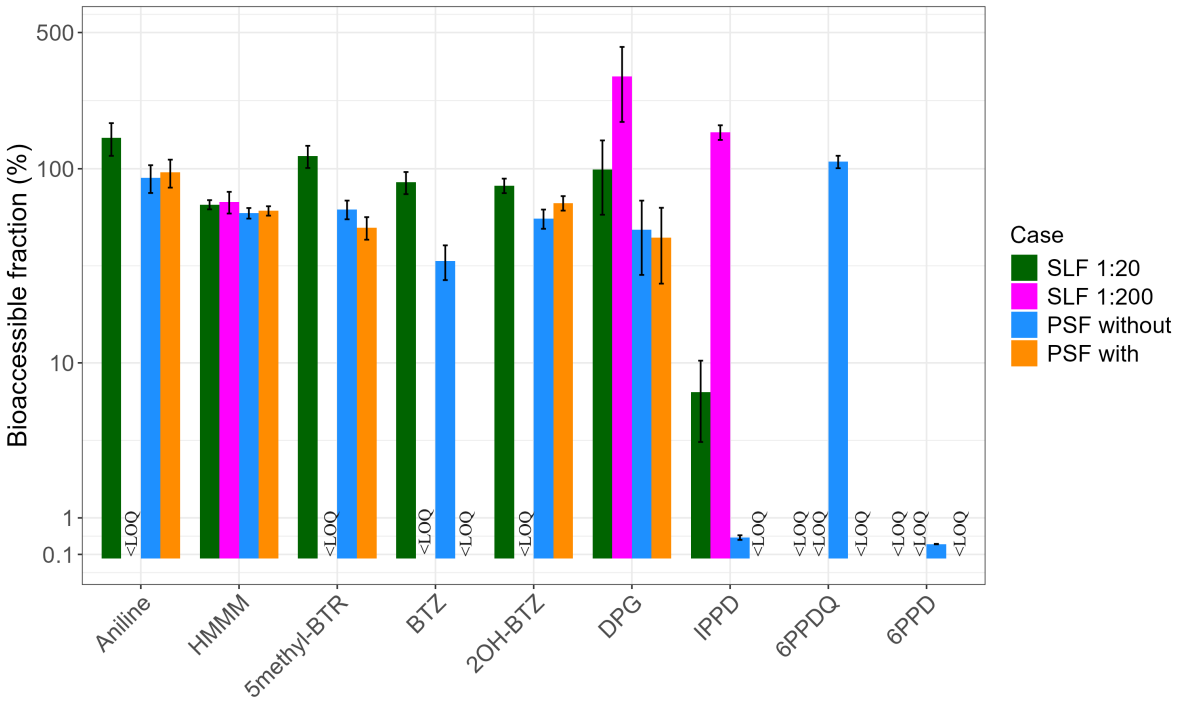

Figure 4.5.: Bioaccessible fractions for climbing hall dust. Fractions were calculated with the time point t = 168 hours for SLF and t = 2 hours for PSF. Compounds are arranged by $\log K_{OW}$ from left to right.

In climbing hall dust, bioaccessible fractions were lower (see Fig. 4.5) Fewer compounds showed values >100 %, due to higher extract concentrations in climbing hall dust. Fig. 4.5 indicates elevated fractions of DPG (297.84 %) and IPPD (153.89 %) at the 1:200 ratio. In contrast, HMMM had consistent fractions (59-65 %) across all fluids. Aniline showed fractions of 144 % in SLF and 95.7 % and 89.7 % in PSF with and without H_2O_2, respectively. Masset et al. reported similar excess aniline values, possibly due to DPG degradation to aniline [26].

Hydrophilic compounds appeared more bioaccessible than hydrophobic ones such as PPDs. The latter are less stable in aqueous media, resulting in lower concentrations in the leachate. For 6PPD and 6PPDQ, results are unreliable, since only one replicate in PSF without H_2O_2 exceeded the LOQ, leading to large uncertainties.

For aniline, BTZ, DPG, 2OH-BTZ, and 5methyl-BTR, bioaccessible fraction was higher in SLF than PSF. This can be a result of the longer exposure times (168 hours in SLF and 2 hours in PSF).

Comparing PSF with and without H_2O_2, similar fractions were observed for aniline (with: 95.70 ± 15.68% and without: 89.70 ± 14.60%) in both fluids. 2OH-BTZ showed slightly higher fractions in the oxidative environment (with: 66.68 ± 5.70% and without: 55.47 ± 6.28%). These compounds are transformation products from DPG and 2SH-BTZ, respectively. DPG showed similar fractions in PSF without (48.57 ± 20.06%) and with H_2O_2 (44.34 ± 18.68%). 5methyl-BTR was slightly higher in PSF without (without: 61.85 ± 6.81% and with: 49.86 ± 6.60%). Previous studies have shown that this compound is likely to be attacked by hydroxyl radicals in the environment of H_2O_2 and degraded, therefore, concentration can be expected to be lower in PSF with H_2O_2 and higher without [66]. The more oxidative environment can contribute to the degradation of the parent compound that are prone to degrade and could lead to a subsequent increase in concentration of the transformation product. Since the concentrations observed here are only marginally higher or similar in both fluids, further investigations are needed to confirm the degradation process.

4.4. Leaching

4.4.1. Influence of Particle Size on Leaching

Differences in particle sizes appear to influence leaching kinetics. When examining leaching results from SLF experiments, road dust and climbing hall dust displayed distinct leaching behaviors. In road dust, DPG release gradually increased over time until reaching a plateau. In contrast, climbing hall dust exhibited an initial rapid release, followed by a more stable concentration over time (see Fig. 4.6).

This trend was similarly observed for aniline across both solid-to-liquid ratios. For 5methyl-BTR, a gradual increase was observed in road dust at both 1:20 and 1:200 ratios, while in climbing hall dust, no values above the LOQ were detected at the 1:200 ratio. In climbing dust, HMMM also showed a rapid release in the 1:20 ratio, however, analysis of this compound in road dust was difficult due to values being near the LOQ.

Conversely, for BTZ and 2amino-BTZ a gradual increase in the climbing hall dust was observed at the 1:20 ratio instead of the instantaneous release observed before. These compounds were not detected at all in the 1:200 ratio and were very low in road dust experiments. This suggests that the slower release in the 1:20 experiment with climbing hall dust may occur since they are present in relatively low concentrations. Leaching is related to the concentration gradient between particles and the fluids, lower concentrations can, therefore, slow down the leaching.

These observed differences between road and climbing hall dust can be attributed to variations in particle size. Smaller particles have a higher surface-to-volume ratio, facilitating faster leaching due to increased particle-fluid contact area. Since climbing hall dust contains finer particles, an instantaneous release is more likely. In contrast, road dust, with larger particles, exhibits a more gradual, continuous release over time. However, rubber particles

are irregularly shaped rather than spherical, which may also influence the leaching behavior, contributing to variability in detected concentrations.

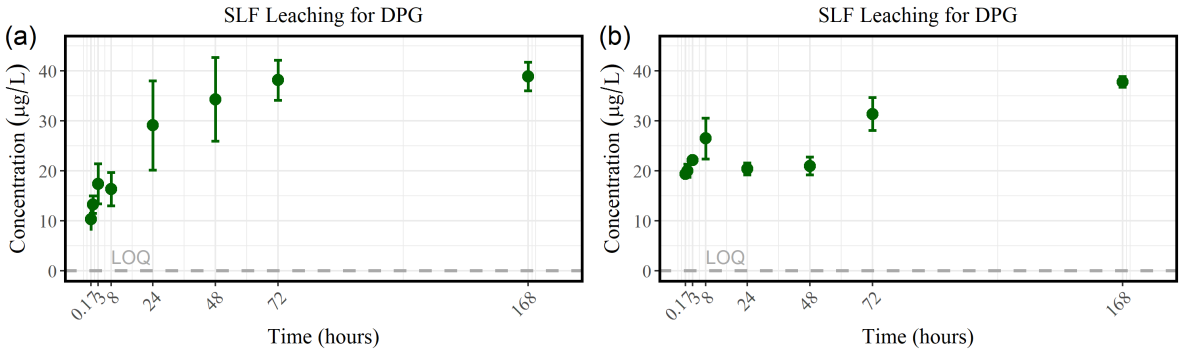

Figure 4.6.: Release kinetics of DPG in SLF at a solid-to-liquid ratio of 1:20 for (a) road dust and (b) climbing hall dust. LOQ values are indicated with dashed lines.

4.4.2. Influence of Solid-to-Liquid Ratios on Leachate Concentrations

In SLF, experiments were performed at two solid-to-liquid ratios: 1:200 and 1:20. Most compounds were detected at both ratios, except for 2amino-BTZ and BTZ, which were not detected in the 1:200 ratio. Some compounds, such as 5methyl-BTR and 2OH-BTZ in climbing hall dust, were sporadically detected or fell below LOQ at 1:200.

When comparing the mean concentrations at the final time point (168 hours), substantial variability was observed between the two ratios. Notably, HMMM showed a near-proportional increase in concentration with increased solid-to-liquid ratio: in climbing hall dust, concentrations rose by a factor of 9.69 (from 0.68 ± 0.08 µg/L to 6.54 ± 0.002 µg/L) when solid-to-liquid ratio was increased ten-fold (see Fig. 4.7).

This is the only compound where the proportional increase in concentration with the solid-to-liquid ratio is observed, all other compounds showed smaller increases.

Other compounds, such as 2OH-BTZ in climbing hall dust and 5methyl-BTR in road dust, showed increases of 6.37 and 5.3 times, respectively. DPG and aniline, showed only relatively minor increases with a higher solid-to-liquid ratio (Fig. 4.8). For example, DPG increased by 3.32 (from 11.34 ± 0.68 µg/L) in climbing hall dust and 1.80 (from 21.58 ± 4.18 µg/L to 38.93 ± 2.83 µg/L) in road dust.

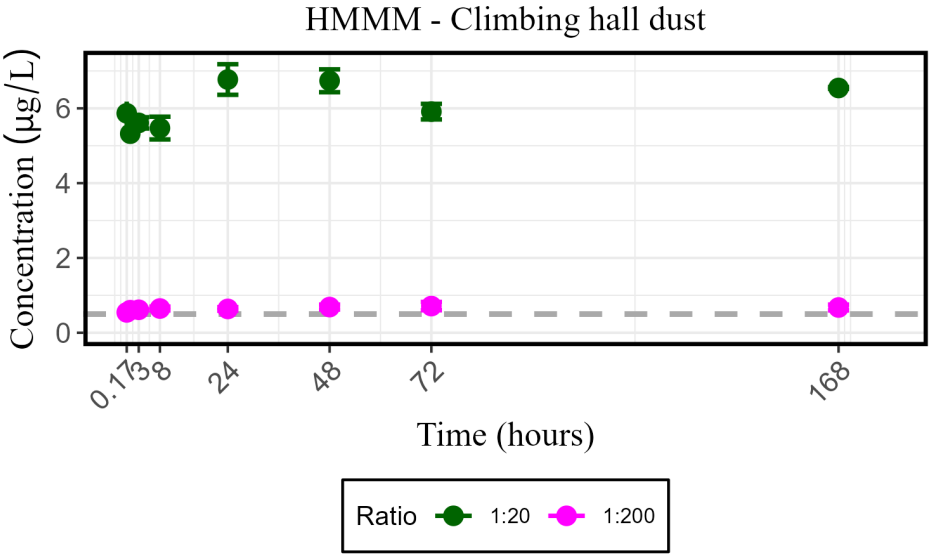

Figure 4.7.: Leaching in SLF for HMMM at solid-to-liquid ratio of 1:200 and 1:20 for climbing hall dust. LOQ values are indicated with dashed lines.

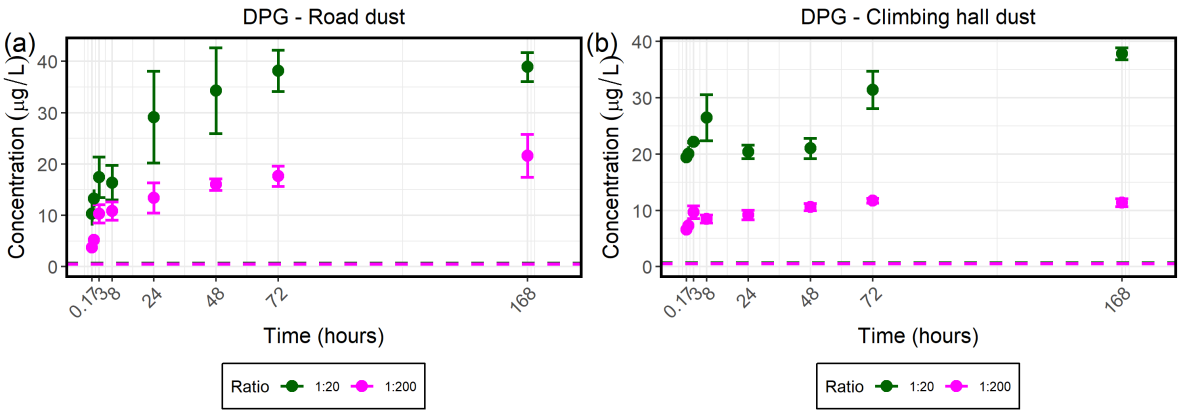

Figure 4.8.: Leaching in SLF for DPG at solid-to-liquid ratio of 1:200 and 1:20 for (a) road dust and (b) climbing hall dust. LOQ values are indicated with dashed lines.

The smaller increases suggest mass transfer limitations or sorption processes may limit concentrations in leachate. Given the high solubility of these compounds (e.g., DPG: 475 mg/L at 20°C, pH = 7 [80]), solubility does not explain the observed concentrations.

One possible explanation is sorption to mineral surfaces. Both road and climbing hall dust contain mineral phases, which can provide sorption sites for organic compounds. Upon leaching out of the rubber particles, the compounds can re-sorb to mineral surfaces, thereby decreasing the detected concentrations. Previous research on the adsorption and removal of Cd(II) from waterlogged paddy soils showed that higher solid-to-liquid ratios result in higher adsorption capacities likely due to more ion binding sites [81]. This would reduce the analyte concentration in solution at higher solid-to-liquid ratios. Additionally, a study on the leaching efficiency of silver revealed that higher solid-to-liquid ratios result in lower leaching rates, which would also reduce the analyte concentration in solution at higher solid-to-liquid ratios. As a possible explanation, they suggested that the higher ratios likely lead to more material that

can agglomerate and hinder leaching [82]. While these studies only looked at metals, similar processes could happen in the present setting with organic compounds.

Another factor to consider is the presence of the pulmonary surfactant (surface active agents) dipalmitoylphosphatidylcholine (DPPC) in SLF . Surfactants can form micelles when their concentration exceeds the critical micelle concentration (CMC). The SLF formulation contains DPPC at 100 mg/L—far above the CMC of 0.0734 mg/L [83]—making micelle formation likely. These micelles can enhance solubility for hydrophobic compounds. However, at higher solid-to-liquid ratios, the amount of compound increases while micelle quantity remains constant, limiting further enhanced solubilization. This could explain the high concentrations in the 1:200 ratio for many compounds (see Fig. 4.5).

4.4.3. Differences in Leaching Kinetics in simulated epithelial and phagolysosomal lung fluid

SLF and PSF exhibit distinct chemical properties. While SLF is slightly alkaline (pH = 8.4), PSF is more acidic (pH = 4.55). The addition of H_2O_2 further increases the reactivity of PSF by creating an oxidative environment.

Leaching experiments were conducted over one week for SLF and over two hours for PSF. This difference reflects the physiological context: particles can remain on the epithelial lung surface for months or years, and a longer period was therefore chosen for SLF. In contrast, in PSF, the engulfment of particles by macrophages and subsequent attack by the formed phagolysosome only takes approximately two hours or less.

Direct comparisons between these fluids are therefore challenging. However, samples were taken from all fluids at two time points — 10 minutes and 1 hour. At 10 minutes, leached concentrations were similar across SLF, PSF without and with H_2O_2, indicating that initial leaching is largely independent of fluid characteristics such as pH (see Fig. 4.9). At the 1 hour time point, concentrations remained comparable (Fig. B3), suggesting that leaching occurs rapidly and is not strongly governed by pH. Instead, compound stability appeared to significantly affect the concentrations in the leachate. Bioaccessible fractions were observed to be higher in SLF for aniline, 5methyl-BTR, BTZ, 2OH-BTZ and DPG (Fig. 4.5) However, since the initial release was similar in both fluids, and subsequent concentration increases were gradual, this confirms that the release process is primarily instantaneous and not strongly dependent on exposure duration. Masset et al. similarly observed that the solubilization potential of polar compounds such as aniline, DPG and BTZs was similar across three different fluids (water, intestinal fluid (pH =7.4) and gastric fluid (pH = 2)), indicating that pH had minimal impact on their solubilization [26].

The stability of each compound varied from fluid to fluid and is therefore important to discuss to understand the observed release kinetics. Therefore, compounds are grouped and discussed based on their stability.

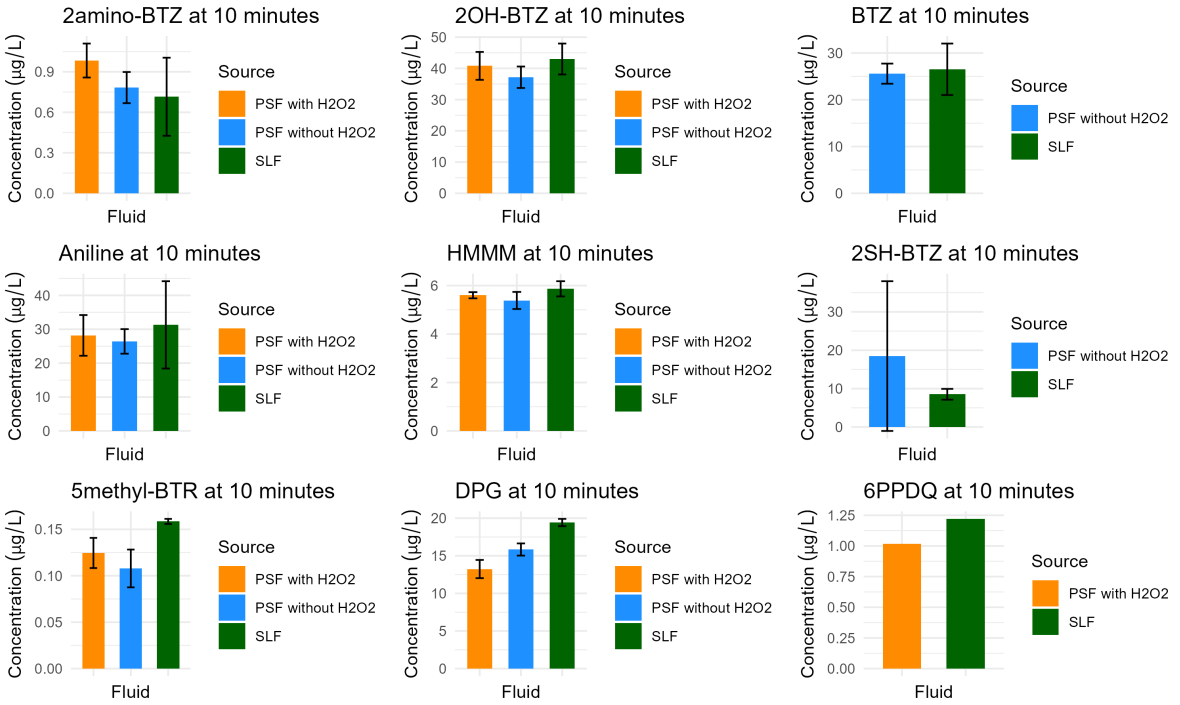

Figure 4.9.: Leached concentrations at 10 minute timepoint in all three fluids for climbing hall dust.

Stable compounds

Some compounds, such as DPG (Fig. 4.10a-b), were stable in all tested fluids. A similar observation was made for aniline (Fig. B7), 5methyl-BTR (Fig. B9) and 2OH-BTZ (Fig. B8).

In SLF, DPG was detected in the stability experiment at 294.32 ± 11.65 µg/L after 10 minutes and stayed consistently at around 300 µg/L with similar standard deviations, despite standards being prepared at 400 µg/L (Fig. 4.10a). This discrepancy may be due to analytical uncertainties or sorption to Eppendorf tube surfaces. A similar pattern was observed for aniline (Fig. B7). Notably, in the mixed-matrix calibration, samples were extracted immediately, whereas in leaching experiments, samples remained in contact with the tubes for at least 10 minutes. Thus, potential sorption during this period was not accounted for.

Despite this, DPG remained stable at approximately 300 µg/L throughout the week, in contrast to previous studies where the biological half-life of DPG in rats was reported to be about 9.6 hours [74]. In both SLF and PSF, DPG was detected at all time points (Fig. 4.10c-d). In contrast, other compounds that did not show 400 µg/L at the first time point were in general largely unstable with rapidly decreasing concentrations, such as CPPD, CPPDQ, IPPD and DPPDQ.

The logD of DPG is -2.77 at pH = 4.55 and 1.06 at pH = 8.4 (see Table 2.2), reflecting a transition from hydrophilic to more lipophilic behavior with increasing pH. This may explain lower concentrations in SLF compared to PSF during stability experiments.

In PSF, compounds leached rapidly and then concentrations plateaued, whereas in SLF, after a similar instant release, leaching still continued to gradually increase over time (Fig. 4.10c-d).

In PSF the release appears to be mostly instantaneous likely due to the shorter time frames, while in SLF, after an initial release, a more continuous increase can be observed.

The observed instantaneous release could be due to the particle sizes. Since respirable dust is used, the particles are very small, thus have a higher surface-to-volume ratio. This facilitates rapid compound diffusion to the particle surface and subsequent leaching. Overall, bioaccessible fractions were higher in SLF compared to PSF which can be related to the longer time frames in SLF and a continuous release, following the rapid initial leaching.

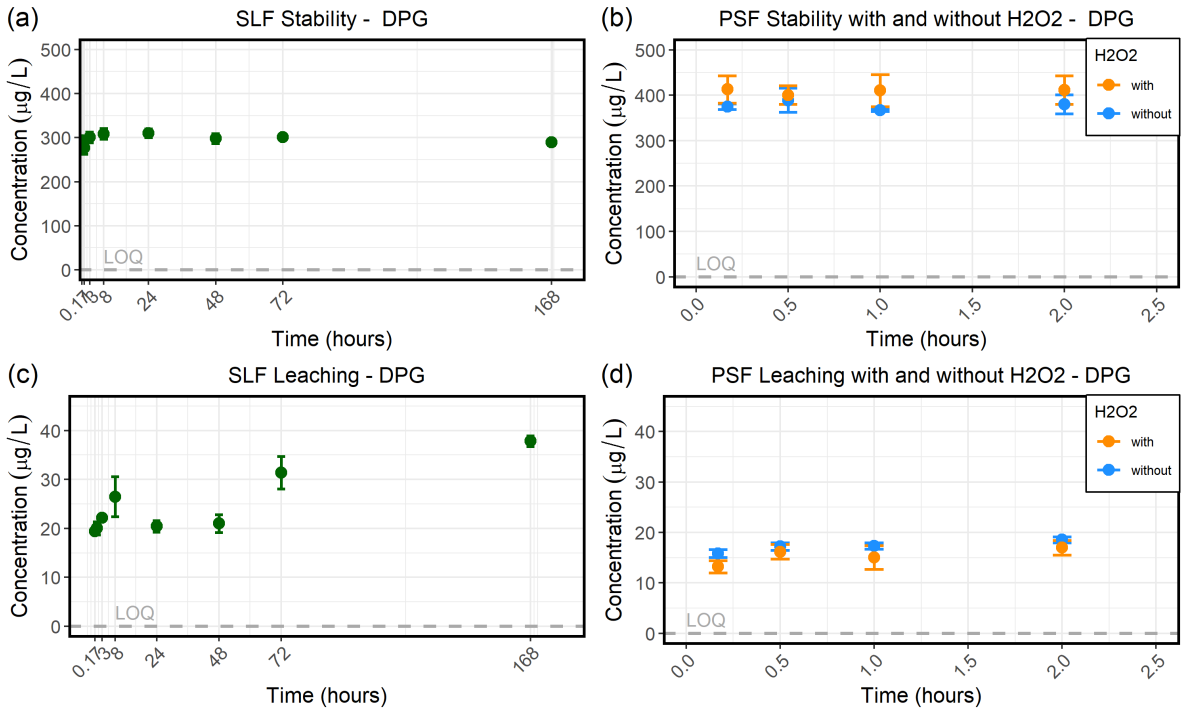

Figure 4.10.: DPG concentrations for climbing hall dust in (a) SLF stability, (b) PSF stability with and without H_2O_2, (c) SLF leaching, and (d) PSF leaching with and without H_2O_2. Grey dashed lines indicate the limit of quantification (LOQ).

Unstable compounds

In contrast to DPG, 2-mercaptobenzothiazole (2SH-BTZ) was unstable in all fluids (Fig. 4.11). In SLF (Fig. 4.11a), its concentration decreased significantly within the first 72 hours and was undetectable by 168 hours. This aligns with previous results on the half-life of 2SH-BTZ in rats, which was reported to be less than 8 hours [75]. Other compounds that showed similar stability trend were IPPD (Fig. B13), CPPD (Fig. B22) and DPPD (Fig. B24).

In PSF stability experiments without H_2O_2, 2SH-BTZ was sporadically detected at low concentrations within the first hour (Fig. 4.11b). However, a blank contamination at the 1-hour and 2-hour time points led to artificially low values. In PSF with H_2O_2, 2SH-BTZ was not detected at all, indicating strong oxidative degradation.

Despite its instability in SLF, 2SH-BTZ was consistently detected in the leachate (Fig. 4.11c),

suggesting continuous release of the compound. Concentrations increased during the first 72 hours, but dropped again by the 168 hour time point. In PSF, it was detected only sporadically without H_2O_2 and not at all in the fluid with H_2O_2. This result is expected, as the oxidative environment of H_2O_2 makes 2SH-BTZ prone to transformations [38, 71].

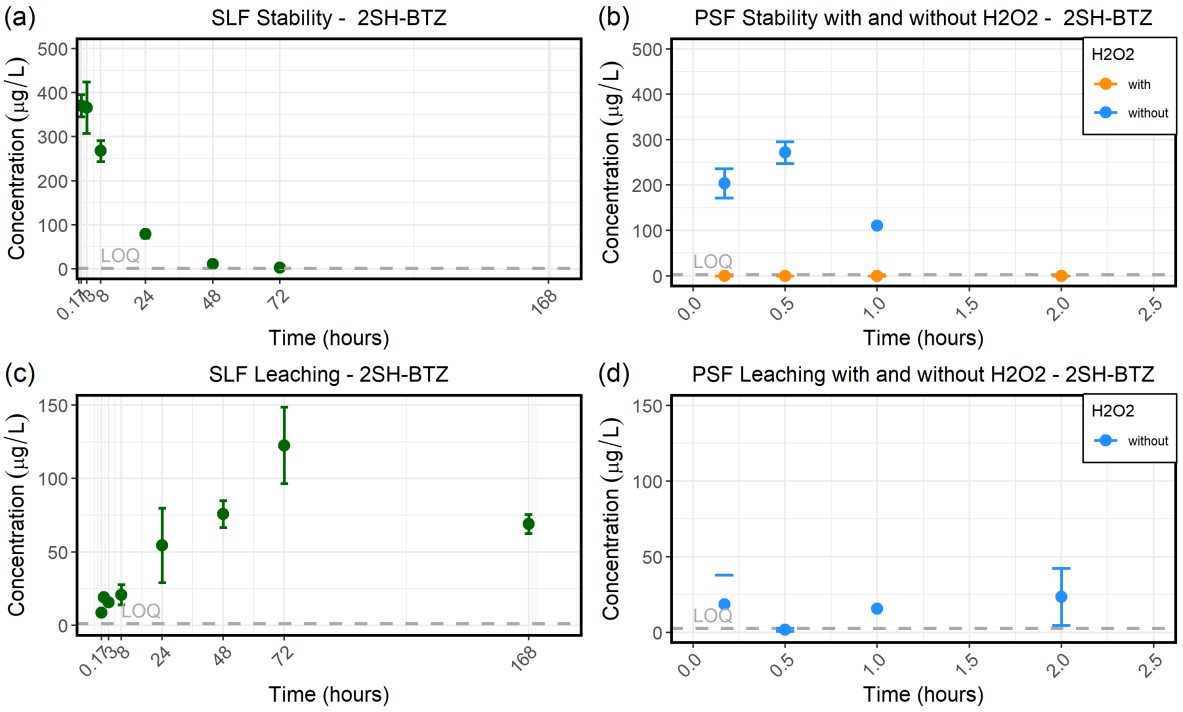

Figure 4.11.: 2SH-BTZ concentrations for climbing hall dust in (a) SLF stability, (b) PSF stability with and without H_2O_2, (c) SLF leaching, and (d) PSF leaching with and without H_2O_2. Grey dashed lines indicate the limit of quantification (LOQ).

Stable in SLF but not PSF

HMMM (Fig. 4.12) showed fluid-specific stability. HMMM was stable in SLF (Fig. 4.12a), but degraded in PSF, particularly in the presence of H_2O_2 (Fig. 4.12b), where its concentration declined more rapidly compared to PSF without H_2O_2.

The logD of HMMM was 0.95 at pH = 4.55 and 1.00 at pH = 8.4, indicating minimal pH-dependent hydrophobicity changes. HMMM was consistently detected in leachates from SLF (Fig. 4.12c) as well as in both PSF fluids (Fig. 4.12d). Notably, in PSF with H_2O_2, concentrations were slightly higher than in the fluid without H_2O_2, despite HMMM's instability in the stability experiments. In all fluids, concentrations stabilized at around 6 µg/L, indicating that even in fluids where the compound degrades, continuous release can be observed. This suggsts that the reactive environment of PSF with H_2O_2 shows an increased leaching even though the compound is unstable in the fluid.

Bioaccessible fractions were comparable across all fluids, ranging from 59 % to 65 %. This indicates that HMMM release occurs at a similar extent regardless of the exposure duration

and does not necessarily increase progressively over time.

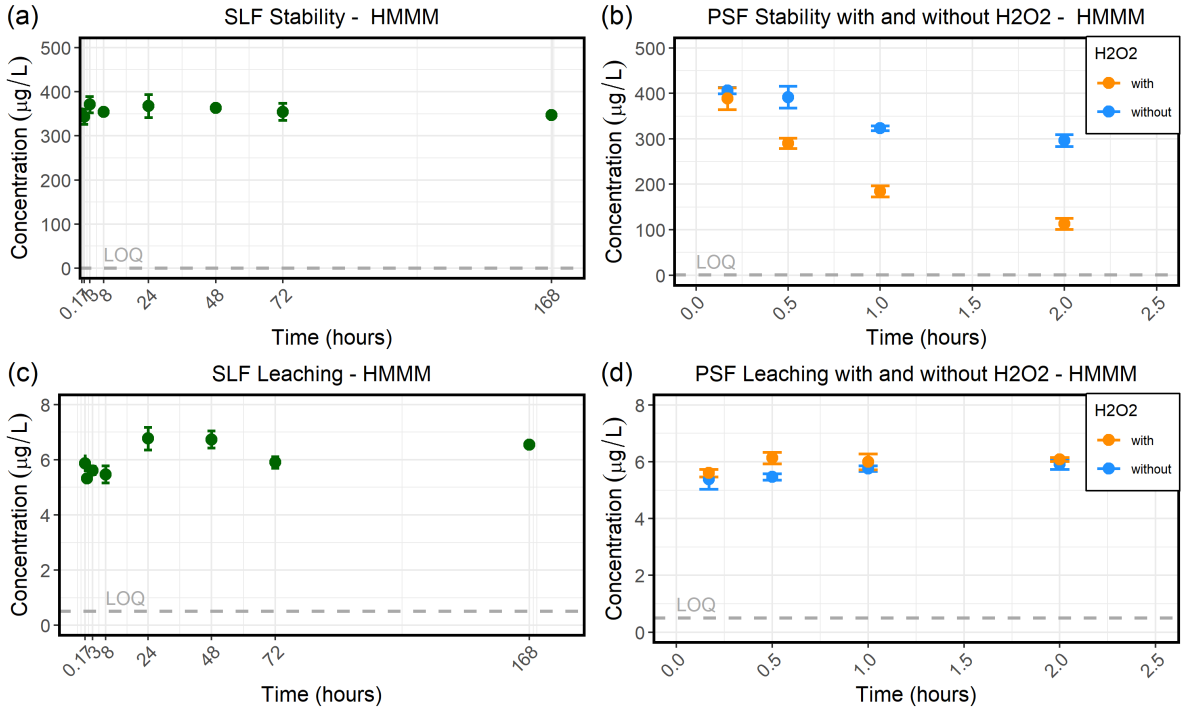

Figure 4.12.: HMMM concentrations for climbing hall dust in (a) SLF stability, (b) PSF stability with and without H_2O_2, (c) SLF leaching, and (d) PSF leaching with and without H_2O_2. Grey dashed lines indicate the limit of quantification (LOQ).

PPDs and quinone derivatives

N,N'substituted p-phenylenediamines (PPDs) and their quinone derivatives are generally hydrophobic and unstable. Stability tests revealed that parent compounds were often much less stable than their quinone products. For example, 6PPD decreased rapidly in the SLF stability experiment and was no longer detected after 48 hours (Fig. 4.13a). In PSF, 6PPD was extremely unstable and detectable only briefly, in the first 30 minutes, in the fluid with H_2O_2 (Fig. 4.13c).

In contrast, the quinone derivative 6PPDQ was significantly more stable in both SLF (Fig. 4.13b) and PSF with and without H_2O_2. Similar trends were observed for CPPD/CPPDQ and IPPD/IPPDQ. This supports previous studies on half-lives of 6PPD and 6PPDQ, identifying the parent to be less stable than the quinone derivative [19, 72, 73]. The increased stability of quinone products in these fluids is concerning, since their toxicity is still largely unknown and 6PPDQ has been shown to be more toxic than its parent compound [19].

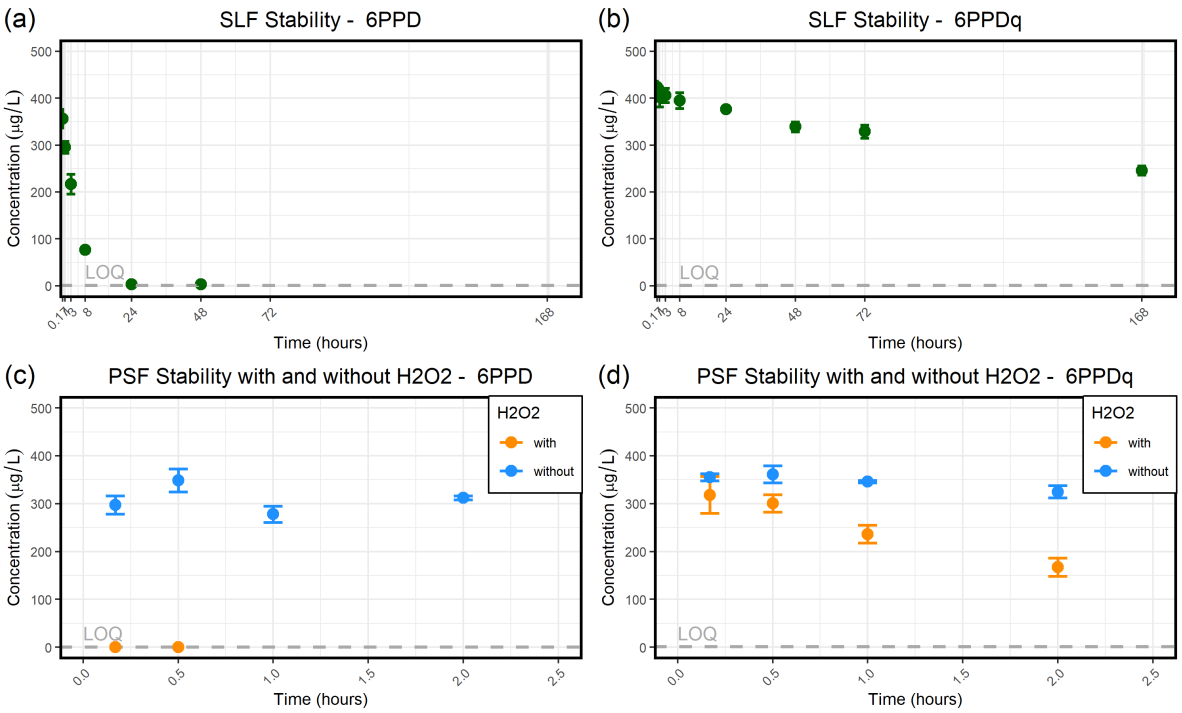

Figure 4.13.: Stability of 6PPD and 6PPDQ in SLF (a,b) and PSF (c,d). Grey dashed lines indicate the limit of quantification (LOQ).

Effect of H_2O_2 on Stability and Leaching

The addition of H_2O_2 creates a highly reactive environment. 2SH-BTZ, for example, is prone to oxidative transformation in this condition. Previously, it has been shown to transform to 2OH-BTZ and BTZ [38, 71].

In PSF, stability experiments revealed that 2OH-BTZ was considerably more stable than its parent compound 2SH-BTZ (Fig. 4.14a-b). While 2SH-BTZ was rapidly degraded, 2OH-BTZ remained stable and constant at around 400 µg/L, regardless of the presence of H_2O_2.

In leaching experiments, 2SH-BTZ was not detected in the fluid with H_2O_2 and only in low concentrations without it. Conversely, 2OH-BTZ was consistently detected in both fluids with concentrations ranging in the fluid with H_2O_2 between 40 and 49 µg/L and without between 37 and 40 µg/L. This supports a likely transformation of 2SH-BTZ to 2OH-BTZ in the fluid with H_2O_2.

Among the compounds tested, stability decreased with H_2O_2 for 2SH-BTZ, 6PPD, 6PPDQ, CPPD, CPPDQ, HMMM, IPPD, and IPPDQ. In contrast, the stability of 2OH-BTZ, 5methyl-BTR, aniline, DPG and BTZ remained largely unaffected. Notably, while BTZ was much more stable in SLF, the detected concentrations increased upon H_2O_2 addition in PSF (Fig. 4.15a-b), consistent with the proposed oxidative transformation pathway from 2SH-BTZ. Since stability tests were done with a mixed- rubber-standard solution, the excess BTZ can likely be formed from 2SH-BTZ.

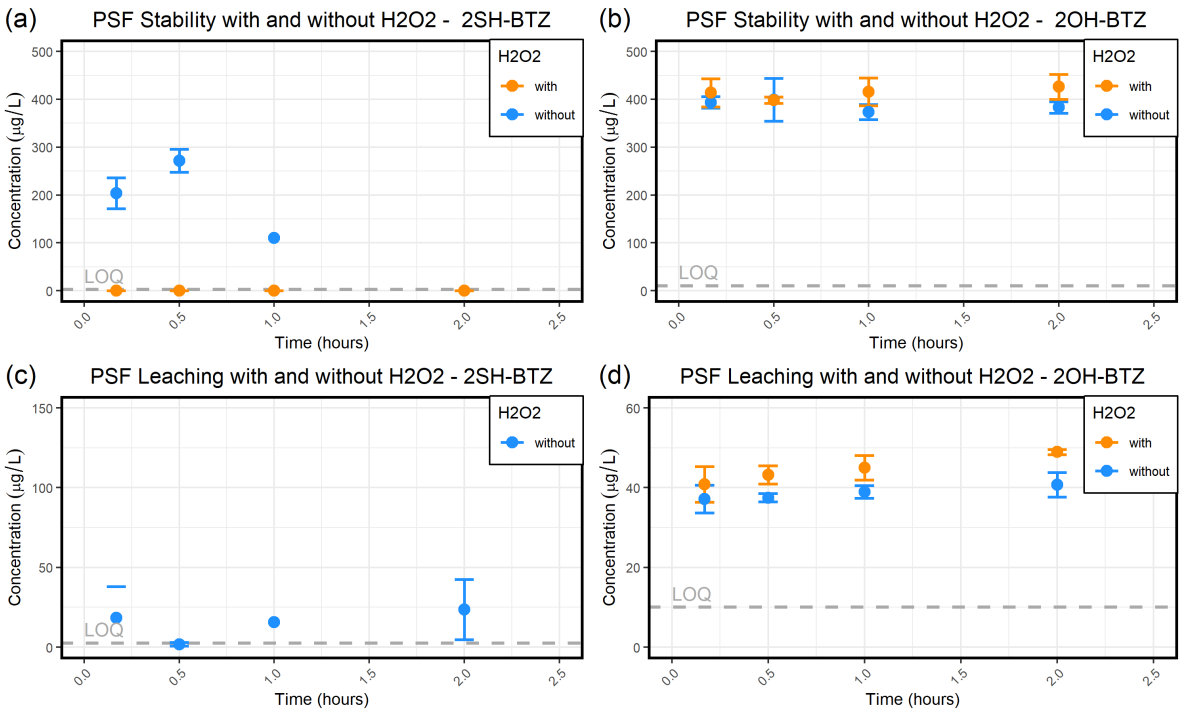

Figure 4.14.: Stability and Leaching of 2SH-BTZ (a,c) and 2OH-BTZ (b-d) in PSF with climbing hall dust. Grey dashed lines indicate the limit of quantification (LOQ).

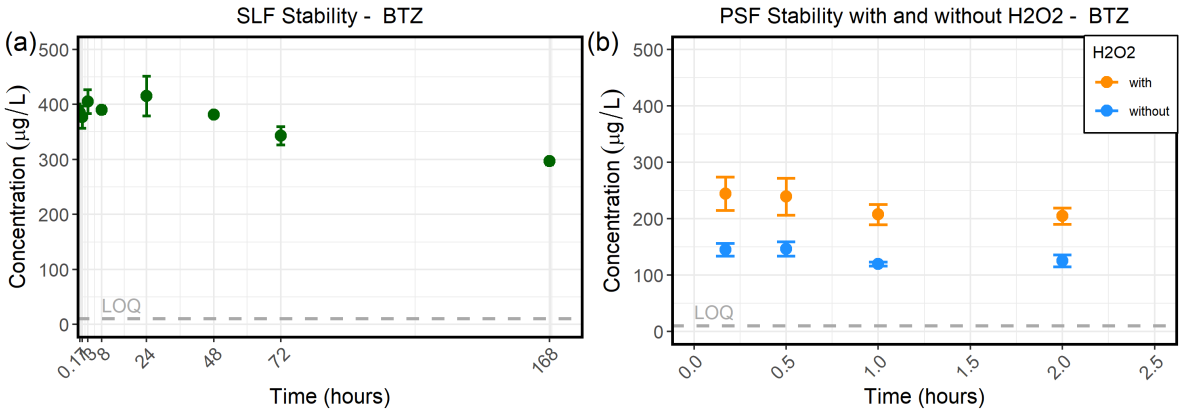

Figure 4.15.: Stability of BTZ in (a) SLF and (b) PSF. Grey dashed lines indicate the limit of quantification (LOQ).

4.5. Release Kinetics

All compounds rapidly leached in both SLF and PSF. The release kinetics of each compound were fitted using a diffusion-controlled and a logarithmic model for both road and climbing hall dust (see Table A9 for all fit parameters). Only stable compounds were included in the modeling, as applying kinetic models to unstable compounds was not meaningful.

Overall, neither model described the leaching behavior particularly well, with most R^2 values falling below 0.7. Table 4.1 summarizes the R^2 values for the two solid-to-liquid ratios in

SLF and both PSF fluids, for five stable compounds. Model fits were generally better for road dust compared to climbing hall dust. This may be due to the slower release kinetics observed in road dust. In contrast, the rapid release from climbing hall dust may have contributed to poorer fits, as the limited early sampling points may not have captured the steep initial release phase. Future experiments could improve model resolution by including additional sampling points at the beginning of the measurement period. Masset et al. found that, when fitting leaching data using the same two models, the R^2 values for most compounds were greater than 0.78, except for the PAHs and for aniline in gastric fluid (R^2 = 0.42). The overall leaching rates for most compounds were much slower than those observed in the present study, which may be explained by the difference in particle size. Masset et al. used larger particles derived from tire tread, which can result in slower leaching compared to the respirable dust fraction examined here [26].

Overall, there were only minor differences between the logarithmic (Log) and diffusion (Diff) models. R^2 were generally comparable between the two, and when one model provided a good fit, the other often did as well. No consistent trends suggest that one model was consistently superior to the other across compounds, fluids, or dust types. This variability likely reflects the compound-specific nature of the release process, influenced by both solution chemistry and dust morphology. Originally, the modeling aimed to relate the estimated rate constants (k-values) to compound properties. However, due to the poor quality of the fits, this analysis was not pursued.

Table 4.1.: Estimated R^2 for fits of road and climbing hall dust in the different fluids and ratios for stable compounds. Diff = Diffusion controlled model, Log = Logarithmic controlled model. Kinetics for compounds below LOQ were not determined (Na). Full table with all fit parameters see Table A9.

Compound	CLIMB								ROAD							
	SLF 1:20		SLF 1:200		PSF without		PSF with		SLF 1:20		SLF 1:200		PSF without		PSF with	
	Diff	Log	Diff	Log	Diff	Log	Diff	Log	Diff	Log	Diff	Log	Diff	Log	Diff	Log
DPG	0.64	0.43	0.63	0.72	0.70	0.71	0.34	0.37	0.76	0.78	0.81	0.84	0.41	0.53	0.70	0.69
Aniline	0.32	0.24	0.02	0.03	NA	NA	NA	NA	0.53	0.64	0.63	0.72	0.39	0.34	0.62	0.59
5methyl-BTR	0.65	0.87	NA	NA	0.38	0.39	NA	NA	0.31	0.41	0.44	0.54	0.53	0.62	0.83	0.78
2OH-BTZ	0.69	0.59	0.14	0.10	0.31	0.28	0.60	0.57	0.46	0.37	NA	NA	NA	NA	0.38	0.28
HMMM	0.35	0.34	0.26	0.36	0.58	0.56	0.29	0.39	0.13	0.21	NA	NA	NA	NA	0.40	0.39

5. Conclusion

Leaching experiments in simulated epithelial lung fluid (SLF) and phagolysosomal lung fluid (PSF) using road and climbing hall dust investigated the release of rubber-derived compounds.

Firstly, it was confirmed that hydrophilic compounds leach more readily, as bioaccessible fractions were highest for aniline, HMMM, 5methyl-BTR, 2OH-BTZ, and DPG, all of which have a $\log K_{OW}$ below 3, which is considered here to be rather hydrophilic.

The hypothesis that parent compounds leach over the course of the week and transformation products are released instantly in SLF was falsified. Instead, most compounds leached rapidly, with only slower gradual increases observed in SLF over extended time frames. Therefore, the location of a compound within the rubber does not appear to govern the release kinetics. Instead, the release appears to be more dominated by particle size. In SLF, no consistent difference in release patterns between parent compounds and their transformation products was observed. If a compound was stable in the fluid, it typically leached quickly, regardless of whether it is a transformation product or a parent compound. A more continuous release was observed for some compounds in road dust compared to climbing hall dust, where release occurred more rapidly. This may be attributed to particle size differences: road dust contained larger particles with a lower surface to volume ratio, likely resulting in slower diffusion and delayed leaching. In general, the rapid release of rubber-derived compounds appears to be associated with finer particles and their larger relative surface area. To further investigate the influence of both particle size and the distribution of compounds within the particle on the release, experiments with samples with equal diameters should be carried out. Minimizing the effect of particle size, allows to focus on how the location of compounds—either on the surface or distributed within the rubber—influences release kinetics.

In PSF, it was hypothesized that the oxidative environment—particularly due to the presence of hydrogen peroxide (H_2O_2)—would promote the degradation of parent compounds such as 2SH-BTZ and PPDs and result in increased levels of their transformation products (2OH-BTZ, BTZ and quinone derivatives) in the leachate. This hypothesis was verified for some compounds. A decreased stability in PSF with H_2O_2 was observed for 2SH-BTZ, 6PPD, 6PPDQ, CPPD, CPPDQ, IPPD and IPPDQ. Notably, 2SH-BTZ was not detected under oxidative conditions, suggesting degradation. Simultaneously, higher concentrations of the transformation products 2OH-BTZ and BTZ were observed in PSF with H_2O_2, while the parent compound 2SH-BTZ was not detected in this fluid, likely due to degradation. Even though stability also decreased for the quinone derivatives of PPDs, the reduction was much smaller than for the parent compound. This supports the hypothesis that the parent compounds are more strongly in-

fluenced by the oxidative environment. Additionally, the parent compound 5methyl-BTR was detected at slightly higher concentrations in the fluid without H_2O_2. 5methyl-BTR is known to degrade under oxidative conditions, which could be a reason for the observed increase in fluid without H_2O_2. Nonetheless, the differences were very small and further investigations are needed to confirm these potential degradation pathways. The presence of H_2O_2 had little to no effect on the stability of certain compounds, including aniline, 2OH-BTZ, 5methyl-BTR, BTZ, and DPG. This suggests that while oxidation enhances degradation for some compounds, other parent compounds and transformation products remain relatively stable in this environment. Additionally, stability experiments showed that many transformation products are generally more stable in the fluids than their parent compounds. This was observed for all PPDs and their quinone derivatives and is consistent with previous findings on the stability of 6PPD and 6PPDQ.

When comparing the leaching behavior across fluids, the measured concentrations in the fluids appeared to be more dependent on the stability of the compound than on pH. However, pH did have an influence in some cases; for example, HMMM was more stable in SLF than in the more acidic PSF, indicating sensitivity to acidic conditions. Overall, concentrations were similar in PSF and SLF at early time points, suggesting that initial leaching is largely independent of fluid chemistry and pH. At later stages, higher concentrations were often observed in SLF, likely due to greater compound stability over time.

Additionally, testing two different solid-to-liquid ratios in SLF revealed that concentrations do not increase proportionally with an increased ratio for all compounds except for HMMM. Only here a proportional increase when the ratio was changed from 1:200 to 1:20 was observed. For all other compounds, the increase was less than tenfold. Several factors may contribute to this, such as potential re-sorption onto dust particles or increased solubility due to micelle formation, which has a capacity that is exceeded at the higher solid-to-liquid ratio.

In summary, the leaching experiments demonstrated that particles from road and climbing hall dust contain rubber-derived compounds, which are rapidly released in simulated lung fluids. Notably, the respirable dust fractions in climbing hall dust revealed a fast release of these compounds, likely due to the high surface-to-volume ratio of these small particles. More investigations of the leaching of rubber-derived compounds from respirable road dust are necessary.

Future research should prioritize repeating these experiments with accurately size-fractionated respirable road dust. If separated properly, a comparison between the two dust types could provide deeper insights into leaching kinetics. Additionally, increasing the number of sampling points within the first 8 hours of measurement may help to capture the rapid release phase more precisely. Additionally, future experiments should further improve the accuracy of the bioaccessible fraction. After leaching, samples should be dried and extracted with ASE to calculate a more accurate bioaccessible fraction.

Beyond leaching experiments, future studies should investigate the toxicity of rubber-derived compounds to human lung cells. Targeted toxicity assessments of specific compounds, as well

as broader, non-targeted toxicity evaluations of road and climbing hall dust, could clarify the implications for respiratory health. Given the widespread use of rubber-derived compounds in many consumer products, understanding their potential impacts on human health is crucial.

6. Bibliography

[1] Kole, P. J., Löhr, A. J., Belleghem, F. G. V., & Ragas, A. M. (2017, October). Wear and tear of tyres: A stealthy source of microplastics in the environment. https://doi.org/10.3390/ijerph14101265

[2] Verschoor, A. (2015). *Towards a definition of microplastics: Considerations for the specification of physico-chemical properties* (Technical Report). National Institute for Public Health and the Environment. Bilthoven, The Netherlands. https://www.rivm.nl/bibliotheek/rapporten/2015-0116.pdf

[3] European Union. (2023). Commission regulation (eu) 2023/2055 of 25 september 2023 amending annex xvii to regulation (ec) no 1907/2006 of the european parliament and of the council concerning the registration, evaluation, authorisation and restriction of chemicals (reach) as regards synthetic polymer microparticles (text with eea relevance). http://data.europa.eu/eli/reg/2023/2055/oj

[4] European Commission and Directorate-General for Environment. (2023). Eu action against microplastics. https://doi.org/10.2779/917472

[5] Statista. (2024a). Global production of plastics from 1950 to 2022 [Accessed: 2024-02-12]. https://www.statista.com/statistics/282732/global-production-of-plastics-since-1950/

[6] European Environment Agency. (2024). Plastics [Accessed: 2024-02-12]. https://www.eea.europa.eu/en/topics/in-depth/plastics?activeTab=07e50b68-8bf2-4641-ba6b-eda1afd544be

[7] Centre, J. R., for Energy, I., Transport, Grigoratos, T., & Martini, G. (2014). *Non-exhaust traffic related emissions - brake and tyre wear pm – literature review*. Publications Office of the European Union. https://doi.org/doi/10.2790/21481

[8] Evangeliou, N., Grythe, H., Klimont, Z., Heyes, C., Eckhardt, S., Lopez-Aparicio, S., & Stohl, A. (2020). Atmospheric transport is a major pathway of microplastics to remote regions. *Nature Communications*, *11*. https://doi.org/10.1038/s41467-020-17201-9

[9] Baensch-Baltruschat, B., Kocher, B., Stock, F., & Reifferscheid, G. (2020). Tyre and road wear particles (trwp) - a review of generation, properties, emissions, human health risk, ecotoxicity, and fate in the environment. *Science of the Total Environment*, *733*. https://doi.org/10.1016/j.scitotenv.2020.137823

[10] Bouredji, A., Pourchez, J., & Forest, V. (2023). Biological effects of tire and road wear particles (trwp) assessed by in vitro and in vivo studies – a systematic review. *Science of The Total Environment*, *894*, 164989. https://doi.org/10.1016/j.scitotenv.2023.164989

[11] United Nations Economic Commission for Europe. (2016). Regulation no 117 of the economic commission for europe of the united nations (unece) — uniform provisions concerning the approval of tyres with regard to rolling sound emissions and/or to adhesion on wet surfaces and/or to rolling resistance [Incorporated into EU law by Commission Regulation (EU) 2016/1350]. http://data.europa.eu/eli/reg/2016/1350/oj

[12] European Parliament and Council of the European Union. (2024). Regulation (eu) 2024/1257 of the european parliament and of the council of 24 april 2024 on type-approval of motor vehicles and engines and of systems, components and separate technical units intended for such vehicles, with respect to their emissions and battery durability (euro 7). http://data.europa.eu/eli/reg/2024/1257/oj

[13] United Nations Economic Commission for Europe. (2024). Ground-breaking new un vehicle regulation to measure tyre abrasion and address microplastics pollution [Accessed: 2025-05-18]. https://unece.org/media/press/388139

[14] Du, B., Liang, B., Li, Y., Shen, M., Liu, L.-Y., & Zeng, L. (2022). First report on the occurrence of n-(1,3-dimethylbutyl)-n'-phenyl-p-phenylenediamine (6ppd) and 6ppd-quinone as pervasive pollutants in human urine from south china. *Environmental Science and Technology Letters*, *9*(12), 1056–1062. https://doi.org/10.1021/acs.estlett.2c00821

[15] Liu, C., Zhao, X., Guo, L., Yu, Q., Zhang, W., Peng, Z., Gao, Y., Gong, X., Li, P., Jiao, H., Zhou, T., Zhang, Q., Song, S., & Jiang, G. (2024). Emerging n-(1,3-dimethylbutyl)-n'-phenyl-p-phenylenediamine (6ppd) and 6ppd quinone in paired human plasma and urine from tianjin, china: Preliminary assessment with demographic factors. *Journal of Hazardous Materials*, *476*, 134818. https://doi.org/10.1016/j.jhazmat.2024.134818

[16] Sommer, F., Dietze, V., Baum, A., Sauer, J., Gilge, S., Maschowski, C., & Gieré, R. (2018). Tire abrasion as a major source of microplastics in the environment. *Aerosol and Air Quality Research*, *18*, 2014–2028. https://doi.org/10.4209/aaqr.2018.03.0099

[17] Johannessen, C., Liggio, J., Zhang, X., Saini, A., & Harner, T. (2022). Composition and transformation chemistry of tire-wear derived organic chemicals and implications for air pollution. *Atmospheric Pollution Research*, *13*. https://doi.org/10.1016/j.apr.2022.101533

[18] Gualtieri, M., Rigamonti, L., Galeotti, V., & Camatini, M. (2005). Toxicity of tire debris extracts on human lung cell line a549. *Toxicology in Vitro*, *19*, 1001–1008. https://doi.org/10.1016/j.tiv.2005.06.038

[19] Tian, Z., Zhao, H., Peter, K. T., Gonzalez, M., Wetzel, J., Wu, C., Hu, X., Prat, J., Mudrock, E., Hettinger, R., Cortina, A. E., Biswas, R. G., Kock, F. V. C., Soong, R., Jenne, A., Du, B., Hou, F., He, H., Lundeen, R., … Kolodziej, E. P. (2021). A ubiquitous tire rubber-derived chemical induces acute mortality in coho salmon. *Science*, *371*(6525), 185–189. https://doi.org/10.1126/science.abd6951

[20] Wagner, S., Funk, C. W., Müller, K., & Raithel, D. J. (2024). The chemical composition and sources of road dust, and of tire and road wear particles–a review. *Science of the Total Environment*, *926*. https://doi.org/10.1016/j.scitotenv.2024.171694

[21] Kreider, M. L., Panko, J. M., McAtee, B. L., Sweet, L. I., & Finley, B. L. (2010a). Physical and chemical characterization of tire-related particles: Comparison of particles generated using different methodologies. *Science of the Total Environment*, *408*, 652–659. https://doi.org/10.1016/j.scitotenv.2009.10.016

[22] Klöckner, P., Seiwert, B., Weyrauch, S., Escher, B. I., Reemtsma, T., & Wagner, S. (2021). Comprehensive characterization of tire and road wear particles in highway tunnel road dust by use of size and density fractionation. *Chemosphere*, *279*. https://doi.org/10.1016/j.chemosphere.2021.130530

[23] Zhang, H. Y., Huang, Z., Liu, Y. H., Hu, L. X., He, L. Y., Liu, Y. S., Zhao, J. L., & Ying, G. G. (2023). Occurrence and risks of 23 tire additives and their transformation products in an urban water system. *Environment International*, *171*. https://doi.org/10.1016/j.envint.2022.107715

[24] Cao, G., Wang, W., Zhang, J., Wu, P., Zhao, X., Yang, Z., Hu, D., & Cai, Z. (2022). New evidence of rubber-derived quinones in water, air, and soil. *Environmental Science and Technology*, *56*, 4142–4150. https://doi.org/10.1021/acs.est.1c07376

[25] Parker, B. W., Beckingham, B. A., Ingram, B. C., Ballenger, J. C., Weinstein, J. E., & Sancho, G. (2020). Microplastic and tire wear particle occurrence in fishes from an urban estuary: Influence of feeding characteristics on exposure risk. *Marine Pollution Bulletin*, *160*, 111539. https://doi.org/10.1016/j.marpolbul.2020.111539

[26] Masset, T., Ferrari, B. J., Dudefoi, W., Schirmer, K., Bergmann, A., Vermeirssen, E., Grandjean, D., Harris, L. C., & Breider, F. (2022). Bioaccessibility of organic compounds associated with tire particles using a fish in vitro digestive model: Solubilization kinetics and effects of food coingestion. *Environmental Science and Technology*, *56*, 15607–15616. https://doi.org/10.1021/acs.est.2c04291

[27] Wik, A., & Dave, G. (2009). Occurrence and effects of tire wear particles in the environment – a critical review and an initial risk assessment. *Environmental Pollution*, *157*(1), 1–11. https://doi.org/10.1016/j.envpol.2008.09.028

[28] World Health Organization. (2021). Global air quality guidelines: Particulate matter (pm2.5 and pm10), ozone, nitrogen dioxide, sulfur dioxide and carbon monoxide. https://www.who.int/publications/i/item/9789240034228

[29] United States Environmental Protection Agency. (2023). Health and environmental effects of particulate matter (pm) [Accessed: 2024-06-26]. https://www.epa.gov/pm-pollution/health-and-environmental-effects-particulate-matter-pm

[30] Tian, L., Zhao, S., Zhang, R., Lv, S., Chen, D., Li, J., Jones, K. C., Sweetman, A. J., Peng, P., & Zhang, G. (2024). Tire wear chemicals in the urban atmosphere: Significant contributions of tire wear particles to pm2.5 [PMID: 39264297]. *Environmental Science & Technology*, *58*(38), 16952–16961. https://doi.org/10.1021/acs.est.4c04378

[31] Clarà, P. C., Jerez, F. R., Ramírez, J. B., & González, C. M. (2023). Deposition and clinical impact of inhaled particles in the lung. *Archivos de Bronconeumología*. https://doi.org/10.1016/j.arbres.2023.01.016

[32] Scheuch, G., Kohlhaeufl, M. J., Brand, P., & Siekmeier, R. (2006, October). Clinical perspectives on pulmonary systemic and macromolecular delivery. https://doi.org/10.1016/j.addr.2006.07.009

[33] Wang, W., Cao, G., Zhang, J., Wu, P., Chen, Y., Chen, Z., Qi, Z., Li, R., Dong, C., & Cai, Z. (2022). Beyond substituted p-phenylenediamine antioxidants: Prevalence of their quinone derivatives in pm2.5. *Environmental Science and Technology*, *56*(15), 10629–10637. https://doi.org/10.1021/acs.est.2c02463

[34] Umweltbundesamt. (2025). Schlechte luftqualität in deutschland. https://www.umweltbundesamt.de/schlechte-luftqualitaet-in-deutschland

[35] Statista. (2024b). Global annual average pm2.5 concentrations 2010-2023 [Accessed: 2025-04-25]. https://www.statista.com/statistics/1464237/global-annual-average-pm25-concentrations/

[36] Salonen, H., Salthammer, T., & Morawska, L. (2020, November). Human exposure to air contaminants in sports environments. https://doi.org/10.1111/ina.12718

[37] Weinbruch, S., Dirsch, T., Ebert, M., Hofmann, H., & Kandler, K. (2008). Dust exposure in indoor climbing halls. *Journal of Environmental Monitoring*, *10*, 648–654. https://doi.org/10.1039/b719344k

[38] Sherman, A., Masset, T., Wimmer, L., Maruschka, L. K., Dailey, L. A., Hüffer, T., Breider, F., & Hofmann, T. (2025). The invisible footprint of climbing shoes: High exposure to rubber additives in indoor facilities. *ACS ES&T Air*, *2*(5), 930–942. https://doi.org/10.1021/acsestair.5c00017

[39] United States Environmental Protection Agency (EPA). (2025). Exposure assessment tools by route [Accessed: 2025-03-17]. https://www.epa.gov/expobox/exposure-assessment-tools-routes

[40] Karlsson, H. L., Ljungman, A. G., Lindbom, J., & Möller, L. (2006). Comparison of genotoxic and inflammatory effects of particles generated by wood combustion, a road simulator and collected from street and subway. *Toxicology Letters*, *165*, 203–211. https://doi.org/10.1016/j.toxlet.2006.04.003

[41] Lindbom, J., Gustafsson, M., Blomqvist, G., Dahl, A., Gudmundsson, A., Swietlicki, E., & Ljungman, A. G. (2007). Wear particles generated from studded tires and pavement induces inflammatory reactions in mouse macrophage cells. *Chemical Research in Toxicology*, *20*, 937–946. https://doi.org/10.1021/tx700018z

[42] Li, Y., Shi, T., Li, X., Sun, H., Xia, X., Ji, X., Zhang, J., Liu, M., Lin, Y., Zhang, R., Zheng, Y., & Tang, J. (2022). Inhaled tire-wear microplastic particles induced pulmonary fibrotic injury via epithelial cytoskeleton rearrangement. *Environment International*, *164*. https://doi.org/10.1016/j.envint.2022.107257

[43] Kreider, M. L., Doyle-Eisele, M., Russell, R. G., McDonald, J. D., & Panko, J. M. (2012). Evaluation of potential for toxicity from subacute inhalation of tire and road wear particles in rats. *Inhalation Toxicology*, *24*, 907–917. https://doi.org/10.3109/08958378.2012.730071

[44] Asimakopoulos, A. G., Wang, L., Thomaidis, N. S., & Kannan, K. (2013). Benzotriazoles and benzothiazoles in human urine from several countries: A perspective on occurrence, biotransformation, and human exposure. *Environment International*, *59*, 274–281. https://doi.org/10.1016/j.envint.2013.06.007

[45] Sorahan, T. (2008). Bladder cancer risks in workers manufacturing chemicals for the rubber industry. *Occupational Medicine (Oxford, England)*, *58*(7), 496–501. https://doi.org/10.1093/occmed/kqn104

[46] Asheim, J., Vike-Jonas, K., Gonzalez, S. V., Lierhagen, S., Venkatraman, V., Veivåg, I. L. S., Snilsberg, B., Flaten, T. P., & Asimakopoulos, A. G. (2019). Benzotriazoles, benzothiazoles and trace elements in an urban road setting in trondheim, norway: Revisiting the chemical markers of traffic pollution. *Science of the Total Environment*, *649*, 703–711. https://doi.org/10.1016/j.scitotenv.2018.08.299

[47] Unice, K. M., Bare, J. L., Kreider, M. L., & Panko, J. M. (2015). Experimental methodology for assessing the environmental fate of organic chemicals in polymer matrices using column leaching studies and oecd 308 water/sediment systems: Application to tire and road wear particles. *Science of the Total Environment*, *533*, 476–487. https://doi.org/10.1016/j.scitotenv.2015.06.053

[48] United States Environmental Protection Agency. (2024). Particle pollution exposure [Retrieved February 6, 2025]. https://www.epa.gov/pmcourse/particle-pollution-exposure

[49] Uribe-Querol, E., & Rosales, C. (2020). Phagocytosis: Our current understanding of a universal biological process. *Frontiers in Immunology*, *11*, 1066. https://doi.org/10.3389/fimmu.2020.01066

[50] Wallenborn, J. G., McGee, J. K., Schladweiler, M. C., Ledbetter, A. D., & Kodavanti, U. P. (2007). Systemic translocation of particulate matter-associated metals following a single intratracheal instillation in rats. *Toxicological Sciences*, *98*, 231–239. https://doi.org/10.1093/toxsci/kfm088

[51] Kastury, F., Smith, E., & Juhasz, A. L. (2017). A critical review of approaches and limitations of inhalation bioavailability and bioaccessibility of metal(loid)s from ambient particulate matter or dust. *Science of the Total Environment*, *574*, 1054–1074. https://doi.org/10.1016/j.scitotenv.2016.09.056

[52] Tomašek, I., Damby, D. E., Stewart, C., Horwell, C. J., Plumlee, G., Ottley, C. J., Delmelle, P., Morman, S., Yazidi, S. E., Claeys, P., Kervyn, M., Elskens, M., & Leermakers, M. (2021). Development of a simulated lung fluid leaching method to assess the release of potentially toxic elements from volcanic ash. *Chemosphere*, *278*. https://doi.org/10.1016/j.chemosphere.2021.130303

[53] Zasadzinski, J., Ding, J., Warriner, H., Bringezu, F., & Waring, A. J. (2001). The physics and physiology of lung surfactants. *Current Opinion in Colloid and Interface Science*, *6*(5), 506–513. https://doi.org/10.1016/S1359-0294(01)00124-8

[54] Kim, K. H., Kabir, E., & Kabir, S. (2015, January). A review on the human health impact of airborne particulate matter. https://doi.org/10.1016/j.envint.2014.10.005

[55] Hampton, M. B., & Dickerhof, N. (2023). Inside the phagosome: A bacterial perspective. *Immunological Reviews*, *314*, 197–209. https://doi.org/10.1111/imr.13182

[56] Stefaniak, A. B., Guilmette, R. A., Day, G. A., Hoover, M. D., Breysse, P. N., & Scripsick, R. C. (2005). Characterization of phagolysosomal simulant fluid for study of beryllium aerosol particle dissolution. *Toxicology in Vitro*, *19*, 123–134. https://doi.org/10.1016/j.tiv.2004.08.001

[57] Hahladakis, J. N., Velis, C. A., Weber, R., Iacovidou, E., & Purnell, P. (2018). An overview of chemical additives present in plastics: Migration, release, fate and environmental impact during their use, disposal and recycling. *Journal of Hazardous Materials*, *344*, 179–199. https://doi.org/10.1016/j.jhazmat.2017.10.014

[58] Huntink, N. (2003, November). *Durability of rubber products: Development of new antidegradants for long-term protection* [PhD Thesis - Research external, graduation UT]. University of Twente. Twente University Press (TUP).

[59] Henkel, C., Hüffer, T., & Hofmann, T. (2022). Polyvinyl chloride microplastics leach phthalates into the aquatic environment over decades. *Environmental Science and Technology*, *56*, 14507–14516. https://doi.org/10.1021/acs.est.2c05108

[60] Turner, A., & Hallett, L. (2012). Bioaccessibility of zinc in estuarine sediment contaminated by tire wear particles. *Water, Air, and Soil Pollution*, *223*, 4889–4894. https://doi.org/10.1007/s11270-012-1244-z

[61] Macklin, C. C. (1955). Lung fluid, alveolar dust drift and initial lesions of disease in the lungs. *Canadian Medical Association Journal*, *72*(9), 664–665.

[62] Wikipedia contributors. (2025). Partition coefficient — Wikipedia, the free encyclopedia [[Online; accessed 31-March-2025]]. https://en.wikipedia.org/wiki/Partition_coefficient

[63] National center for biotechnology information. pubchem compound database [accessed on 12.06.2024]. (n.d.). https://pubchem.ncbi.nlm.nih.gov/

[64] Perrin, D. D. (1972). *Dissociation constants of organic bases in aqueous solution: Supplement 1972*. Butterworths.

[65] Liao, C., Kim, U. J., & Kannan, K. (2018). A review of environmental occurrence, fate, exposure, and toxicity of benzothiazoles. *Environmental Science and Technology*, *52*, 5007–5026. https://doi.org/10.1021/acs.est.7b05493

[66] Bahnmüller, S., Loi, C. H., Linge, K. L., von Gunten, U., & Canonica, S. (2015). Degradation rates of benzotriazoles and benzothiazoles under uv-c irradiation and the advanced oxidation process uv/h_2o_2. *Water Research*, *74*, 143–154. https://doi.org/10.1016/j.watres.2014.12.039

[67] Kodešová, R., Fedorova, G., Kodeš, V., Kočárek, M., Rieznyk, O., Fér, M., Švecová, H., Klement, A., Bořík, A., Nikodem, A., & Grabic, R. (2023). Assessment of potential mobility of selected micropollutants in agricultural soils of the czech republic using their sorption predicted from soil properties. *Science of the Total Environment*, *865*. https://doi.org/10.1016/j.scitotenv.2022.161174

[68] European Chemicals Agency (ECHA). (2025a). Partition coefficient (n-octanol/water) - registered dossier for substance [[Accessed 31-March-2025]]. https://echa.europa.eu/sk/registration-dossier/-/registered-dossier/14992/4/8

[69] Tang, T., & Kolodziej, E. P. (2022). Sorption and desorption of tire rubber and roadway-derived organic contaminants in soils and a representative engineered geomedium. *Environmental Science and Technology Water*, *2*(12), 2623–2633.

[70] Hu, X., Zhao, H. N., Tian, Z., Peter, K. T., Dodd, M. C., & Kolodziej, E. P. (2022). Transformation product formation upon heterogeneous ozonation of the tire rubber antioxidant 6ppd (n-(1,3-dimethylbutyl)-n'-phenyl-p-phenylenediamine). *Environmental science & technology letters*, *9*(5), 413–419.

[71] Derco, J., Kassai, A., Melicher, M., & Dudas, J. (2014). Removal of the 2-mercaptobenotiazole from model wastewater by ozonation. *The Scientific World Journal*, *2014*(1), 173010. https://doi.org/10.1155/2014/173010

[72] European Chemicals Agency (ECHA). (2021). Echa registration-dossier n-1,3-dimethylbutyl-n'-phenyl-p-phenylenediamine, endpoint summary, studies with ppds (6ppd, 7ppd, 77pd, 44pd) (allmendinger 2012) [Accessed: 2025-03-17]. https://echa.europa.eu/de/registration-dossier/-/registered-dossier/15367/6/2/1

[73] Hiki, K., Asahina, K., Kato, K., Yamagishi, T., Omagari, R., Iwasaki, Y., Watanabe, H., & Yamamoto, H. (2021). Acute toxicity of a tire rubber-derived chemical, 6ppd quinone, to freshwater fish and crustacean species. *Environmental Science and Technology Letters*, *8*(9), 779–784.

[74] Ioannou, Y., & Matthews, H. (1984). Absorption, distribution, metabolism, and excretion of 1,3-diphenylguanidine in the male f344 rat. *Fundamental and Applied Toxicology*, *4*(1), 22–29. https://doi.org/10.1016/0272-0590(84)90216-1

[75] National Toxicology Program. (1988). *Ntp toxicology and carcinogenesis studies of 2-mercaptobenzothiazole (cas no. 149-30-4) in f344/n rats and b6c3f1 mice (gavage studies)* (tech. rep. No. 332) (PMID: 12732904). National Toxicology Program. http://ntp.niehs.nih.gov/ntp/htdocs/lt_rpts/tr332.pdf

[76] Gamble, J. L. (1941). *Chemical anatomy, physiology and pathology of extracellular fluid: A lecture syllabus*. Department of Pediatrics, Harvard Medical School.

[77] Kreider, M. L., Panko, J. M., McAtee, B. L., Sweet, L. I., & Finley, B. L. (2010b). Physical and chemical characterization of tire-related particles: Comparison of particles generated using different methodologies. *Science of The Total Environment*, *408*(3), 652–659. https://doi.org/10.1016/j.scitotenv.2009.10.016

[78] Deng, C., Huang, J., Qi, Y., Chen, D., & Huang, W. (2022). Distribution patterns of rubber tire-related chemicals with particle size in road and indoor parking lot dust. *Science of the Total Environment*, *844*. https://doi.org/10.1016/j.scitotenv.2022.157144

[79] Huang, W., Shi, Y., Huang, J., Deng, C., Tang, S., Liu, X., & Chen, D. (2021). Occurrence of substituted p-phenylenediamine antioxidants in dusts. *Environmental Science and Technology Letters*, *8*, 381–385. https://doi.org/10.1021/acs.estlett.1c00148

[80] European Chemicals Agency (ECHA). (2025b). Registration dossier: DPG [Accessed: 2025-01-14]. https://echa.europa.eu/registration-dossier/-/registered-dossier/14992/4/9#:~:text=The%20water%20solubility%20of%20DPG%20was%20estimated%20at%20475%20mg,is%20very%20soluble%20in%20water.

[81] Wu, M., Liu, H., & Yang, C. (2019). Effects of pretreatment methods of wheat straw on adsorption of cd(ii) from waterlogged paddy soil. *International Journal of Environmental Research and Public Health*, *16*(2). https://doi.org/10.3390/ijerph16020205

[82] Tian, J., Wu, D., Li, S., Ma, W., & Wang, R. (2024). Effect of process variables on leaching behavior and kinetics of silver element from waste photovoltaic modules. *Separation and Purification Technology*, *335*. https://doi.org/10.1016/j.seppur.2023.126062

[83] Smith, R., & Tanford, C. (1972). The critical micelle concentration of l-α- dipalmitoylphosphatidylcholine in water and water/methanol solutions. *Journal of Molecular Biology*, *67*(1), 75–83. https://doi.org/10.1016/0022-2836(72)90387-7

Appendix

A. Tables

Table A1.: Simulated epithelial lung fluid [52].

Compound	Final Concentration (mg/L)
NaCl	6400
$CaCl_2$•$2H_2O$	255
Na_2HPO_4	150
$NaHCO_3$	2700
NH_4Cl	118
$MgCl_2$•$6H_2O$	212
Na_2SO_4•$10H_2O$	179
Na_3citrate•$2H_2O$	160
Glycine	190
Dipalmitoylphosphatidylcholine (DPPC)	100

Table A2.: Phagolysosomal fluid [56].

Compound	Final Concentration (mg/L)
Na_2HPO_4	142
NaCl	6650
Na_2SO_4	71
$CaCl_2$•$2H_2O$	29
Glycine	450
Potassium hydrogen phthalate	4084.6
Alkylbenzyldimethylammonium chloride (ABDC)	50
H_2O_2 *for PSF with*	2900

Formula for calculation of the error propagation for bioaccessible fraction

$$SD_{bioaccessible} = bioaccessible * \sqrt{\left(\frac{SD_{C_{Leached}}}{C_{Leached}}\right)^2 + \left(\frac{SD_{C_{Extracted}}}{C_{Extracted}}\right)^2}. \quad \text{(A1)}$$

Table A3.: Parameters for Calculating D50 values for stages of the NGI between 30 L/min and 100 L/min.

Stage	D50 at 60 L/min (μm)	X
1	8.06	0.54
2	4.46	0.52
3	2.82	0.50
4	1.66	0.47
5	0.94	0.53
6	0.55	0.60
7	0.34	0.67

Table A4.: Extraction recovery for dust samples. Compounds were spiked into ASE cells and extracted following the protocol described in the Methods section. Absolute recovery refers to measurements without internal standard correction, while relative recovery accounts for internal standard correction. (Tested and provided by Anya Sherman)

Compound	**Absolute recovery (%) mean ± SD**	**Relative recovery (%) mean ± SD**
Aniline	62 ± 29	66 ± 22
BTZ	96 ± 3	98 ± 4
2amino-BTZ	100 ± 4	98 ± 4
2OH-BTZ	87 ± 4	89 ± 5
2SH-BTZ	29 ± 11	32 ± 14
6PPDQ	73 ± 24	97 ± 6
DPG	65 ± 26	76 ± 20
6PPD	73 ± 20	87 ± 10
HMMM	107 ± 5	145 ± 34
CPPD	82 ± 23	101 ± 7
CPPDQ	78 ± 16	109 ± 9
IPPD	77 ± 19	90 ± 9
IPPDQ	84 ± 11	117 ± 18
DPPD	102 ± 21	132 ± 7
DPPDQ	62 ± 27	74 ± 21

Table A5.: LOQ Values for Different Compounds: Stock solutions were never used more than one month after preparation. The UPLC-MS/MS instrument was internally calibrated weekly. Despite this, instrument drift likely introduced variability. Both stock stability and fluctuations in instrument sensitivity likely resulted in variations of the LOQ.

Compound	LOQ SLF 1:20	LOQ SLF 1:200	LOQ PSF Stability and Leaching	LOQ SLF Stability
Aniline	25	7.5	50	25
2amino-BTZ	1	0.5	0.5	1
DPG	0.64	0.5	0.01	3.88
5methyl-BTR	0.05	0.05	0.01	0.05
IPPDQ	0.05	0.1	0.01	0.05
2OH-BTZ	10	10	10	10
BTZ	10	10	10	10
2SH-BTZ	1	10	2.5	1
CPPDQ	0.5	0.5	0.1	0.5
6PPD	1	1	0.05	1
HMMM	0.5	0.5	0.5	0.5
IPPDQ	0.5	0.5	0.5	0.5
DPPDQ	1	10	0.5	1
CPPDQ	0.5	2.5	0.5	0.5
6PPDQ	0.5	0.5	0.5	0.5
DPPD	5	7.5	0.5	5

Table A6.: R^2 of the calibration curves in the different experiments.

Compound	R^2 for SLF 1:20 and stability	R^2 for PSF leaching and stability	R^2 for SLF 1:200
2amino-BTZ	0.966	0.963	0.992
DPG	0.999	0.998	0.999
Aniline	0.970	0.951	0.995
5methyl-BTR	0.999	0.996	0.999
2OH-BTZ	0.994	0.995	0.994
IPPD	0.994	0.996	0.989
BTZ	0.993	0.986	0.991
2SH-BTZ	0.955	0.998	0.977
HMMM	0.997	0.997	0.999
CPPD	0.978	0.998	0.979
6PPD	0.965	0.996	0.964
IPPDQ	0.999	0.998	1.000
DPPDQ	0.988	0.982	0.998
CPPDQ	0.996	0.985	0.990
6PPDQ	0.995	0.999	0.995
DPPD	0.992	0.983	0.990

Table A7.: MRM Parameters for Targeted Compounds.

Compound Name	Surrogate standard	Precursor Ion m/z	Product Ion m/z	Fragmentor Voltage (V)	Collision Energy (V)	Cell Acc (V)	RT (min)
2amino-BTZ	**d4-BTZ**	**151**	**109**	**150**	**30**	**5**	**40**
2amino-BTZ		151	65	150	38	5	40
2OH-BTZ	**d4-BTZ**	**152**	**124**	**140**	**22**	**4**	**40**
2OH-BTZ		152	92	140	26	4	40
2SH-BTZ	**d4-BTZ**	**168**	**135**	**135**	**28**	**5**	**40**
2SH-BTZ		168	124	135	24	5	40
2SH-BTZ		168	109	135	28	5	40
5methyl-BTR	**d4-BTZ**	**134.1**	**77.1**	**108**	**31**	**5**	**40**
5methyl-BTR		134.1	79.1	108	23	5	40
5methyl-BTR		134.1	51.2	108	45	5	40
6PPD	**d5-6PPDQ**	**269**	**184**	**150**	**45**	**5**	**40**
6PPD		269	107	150	45	5	40
6PPD		269	93	150	45	5	40
6PPDQ	**d5-6PPDQ**	**299**	**187**	**150**	**30**	**5**	**40**
6PPDQ		299	215	150	30	5	40
6PPDQ		299	241	150	53	5	40
Aniline	**d4-BTZ**	**94**	**77**	**100**	**22**	**4**	**40**
Aniline		94	51	100	23	4	40
Aniline		94	50	100	41	4	40
BTZ	**d4-BTZ**	**136**	**109**	**150**	**31**	**5**	**40**
BTZ		136	77	150	27	5	40
BTZ		136	65	150	38	5	40
d4-BTZ		**140**	**69**	**150**	**36**	**5**	**40**
d4-BTZ		140	81	150	19	5	40
d4-BTZ		140	113	150	31	5	40
CPPD	**d5-6PPDQ**	**267.2**	**184**	**100**	**30**	**5**	**40**
CPPD		267.2	107	100	50	5	40
CPPD		267.2	93.1	100	46	5	40
CPPDQ	**d5-6PPDQ**	**297.1**	**187**	**130**	**34**	**5**	**40**
CPPDQ		297.1	215	130	18	5	40
CPPDQ		297.1	55.2	130	50	5	40
d5-6PPDQ		**304.2**	**246.1**	**110**	**36**	**4**	**40**
d5-6PPDQ		304.2	192.1	110	36	5	40
d5-6PPDQ		304.2	220.1	110	36	5	40
DPG	**d5-6PPDQ**	**212**	**119**	**150**	**20**	**5**	**40**
DPG		212	195	150	20	5	40
DPG		212	94	150	20	5	40
DPPD	**d5-6PPDQ**	**260.1**	**183**	**130**	**38**	**5**	**40**
DPPD		260.1	156	130	46	5	40
DPPD		260.1	167	130	46	5	40
DPPDQ	**d5-6PPDQ**	**291.1**	**263**	**150**	**22**	**5**	**40**
DPPDQ		291.1	144	150	38	5	40
DPPDQ		291.1	235.2	150	34	5	40
HMMM	**d4-BTZ**	**391**	**177**	**150**	**35**	**5**	**40**
HMMM		391	283	150	15	5	40
HMMM		391	253	150	23	5	40
HMMM		391	207	150	19	5	40
IPPD	**d5-6PPDQ**	**227.2**	**184**	**100**	**18**	**5**	**40**
IPPD		227.2	107	100	46	5	40
IPPD		227.2	118	100	46	5	40
IPPDQ	**d5-6PPDQ**	**257.2**	**187**	**110**	**30**	**5**	**40**
IPPDQ		257.2	216	110	30	5	40
IPPDQ		257.2	170	110	34	5	40

Table A8.: Preliminary tests at different solid-to-liquid ratios of road and climbing hall dust in SLF after 72 hours of leaching (ratios of 1:2000, 1:1000 and 1:200).

Sample/Compound	Aniline	BTZ	CPPD	CPPDQ	DPG	DPPD	DPPDQ	HMMM	IPPD	IPPDQ	2amino-BTZ	2OH-BTZ	2SH-BTZ	5-methyl-BTR	6PPDQ	6PPD
climb_1_2000_B	0.27	<LOQ	<LOQ	<LOQ	<LOQ	<LOQ	<LOQ	<LOQ	<LOQ	<LOQ	<LOQ	<LOQ	<LOQ	<LOQ	<LOQ	<LOQ
climb_1_1000_C	0.17	<LOQ	<LOQ	<LOQ	<LOQ	<LOQ	<LOQ	<LOQ	<LOQ	<LOQ	<LOQ	<LOQ	<LOQ	<LOQ	<LOQ	<LOQ
climb_1_200_A	0.11	3.70	<LOQ	<LOQ	<LOQ	<LOQ	<LOQ	0.00	<LOQ	<LOQ	0.00	3.45	5.51	<LOQ	<LOQ	<LOQ
climb_1_200_B	0.11	6.61	<LOQ	<LOQ	<LOQ	<LOQ	<LOQ	0.25	<LOQ	<LOQ	0.65	5.72	12.91	<LOQ	<LOQ	<LOQ
road_1_2000_A	0.53	<LOQ	<LOQ	<LOQ	8.71	<LOQ	<LOQ	<LOQ	<LOQ	<LOQ	<LOQ	<LOQ	<LOQ	<LOQ	<LOQ	<LOQ
road_1_2000_B	1.24	<LOQ	<LOQ	<LOQ	9.02	<LOQ	<LOQ	<LOQ	<LOQ	<LOQ	<LOQ	<LOQ	<LOQ	<LOQ	<LOQ	<LOQ
road_1_1000_A	0.59	<LOQ	<LOQ	<LOQ	<LOQ	<LOQ	<LOQ	<LOQ	<LOQ	<LOQ	<LOQ	<LOQ	<LOQ	<LOQ	<LOQ	<LOQ
road_1_1000_C	0.82	<LOQ	<LOQ	<LOQ	8.84	<LOQ	<LOQ	<LOQ	<LOQ	<LOQ	<LOQ	<LOQ	<LOQ	<LOQ	<LOQ	<LOQ
road_1_200_B	0.48	3.66	<LOQ	<LOQ	<LOQ	<LOQ	<LOQ	<LOQ	<LOQ	<LOQ	<LOQ	<LOQ	13.17	<LOQ	<LOQ	<LOQ
road_1_200_C	0.53	0.00	<LOQ	<LOQ	<LOQ	<LOQ	<LOQ	<LOQ	<LOQ	<LOQ	<LOQ	<LOQ	0.00	<LOQ	<LOQ	<LOQ

Table A9.: Fit parameters of road and climbing hall dust in the different fluids and ratios for stable compounds. Diff = Diffusion controlled model, Log = logarithmic controlled model. Kinetics for compounds below LOQ were not determined (NA).

Compound		DPG		Aniline		5methyl-BTR		2OH-BTZ		HMMM	
Climb 1:20	Model	Diff	Log	Diff	Log	Diff	Log	Diff	Log	Diff	Log
	Formula	$C(t) = 18.59 - 1.28 * \sqrt{t}$	$C(t) = 20.18 + 2.05 * log(t)$	$C(t) = 29.67 - 1.30 * \sqrt{t}$	$C(t) = 31.02 + 2.24 * log(t)$	$C(t) = 0.20 - 0.01 * \sqrt{t}$	$C(t) = 0.12 + 0.02 * log(t)$	$C(t) = 40.29 - 1.70 * \sqrt{t}$	$C(t) = 42.12 + 2.91 * log(t)$	$C(t) = 5.62 - 0.09 * \sqrt{t}$	$C(t) = 5.69 + 0.15 * log(t)$
	Estimated k	1.28	2.05	1.30	2.24	0.01	0.02	1.70	2.91	0.08	0.15
	AIC	133.76	144.03	152.55	154.71	-94.69	-119.03	147.38	153.93	37.58	38.07
	R^2	0.64	0.43	0.32	0.24	0.65	0.87	0.69	0.59	0.35	0.34
	p-value	5.03E-06	6.47E-04	7.76E-03	2.29E-02	1.97E-06	2.47E-11	4.87E-07	1.05E-05	2.32E-03	2.96E-03
	95% CI (Lower,Upper)	(0.84,1.72)	(0.99,3.12)	(0.39,2.22)	(0.35,4.13)	(0.01,0.01)	(0.02,0.03)	(1.20,2.20)	(1.85,3.97)	(0.03,0.14)	(0.06,0.25)
Climb 1:200	Formula	$C(t) = 7.687 - 0.350 * \sqrt{t}$	$C(t) = 7.769 + 0.716 * log(t)$	$C(t) = 10.058 - 0.038 * \sqrt{t}$	$C(t) = 10.045 + 0.087 * log(t)$	NA	NA	$C(t) = 6.097 - 0.200 * \sqrt{t}$	$C(t) = 6.059 + 0.401 * log(t)$	$C(t) = 0.592 - 0.010 * \sqrt{t}$	$C(t) = 0.593 + 0.021 * log(t)$
	Estimated k	0.35	0.72	0.04	0.09	NA	NA	0.20	0.40	0.01	0.02
	AIC	117.41	106.91	124.71	124.38	NA	NA	127.33	128.73	-93.71	-99.68
	R^2	0.63	0.72	0.02	0.03	NA	NA	0.14	0.10	0.26	0.36
	p-value	4.95E-09	3.24E-11	4.08E-01	3.18E-01	NA	NA	3.87E-02	8.37E-02	9.75E-04	4.95E-05
	95% CI (Lower,Upper)	(0.26,0.44)	(0.56,0.87)	(-0.05,0.13)	(-0.09,0.26)	NA	NA	(0.01,0.39)	(-0.06,0.86)	(0.00,0.02)	(0.01,0.03)
Climb PSF without	Formula	$C(t) = 15.01 - 2.53 * \sqrt{t}$	$C(t) = 17.71 + 1.04 * log(t)$	$C(t) = 26.41 + 0.16 * \sqrt{t}$	$C(t) = 26.23 - 0.09 * log(t)$	$C(t) = 0.08 - 0.07 * \sqrt{t}$	$C(t) = 0.145 + 0.03 * log(t)$	$C(t) = 35.30 - 3.74 * \sqrt{t}$	$C(t) = 39.24 + 1.44 * log(t)$	$C(t) = 5.13 - 0.57 * \sqrt{t}$	$C(t) = 5.73 + 0.23 * log(t)$
	Estimated k	2.53	1.04	-0.16	-0.09	0.07	0.03	3.74	1.44	0.57	0.23
	AIC	28.58	28.10	38.49	38.48	-42.84	-43.05	57.38	57.91	-1.26	-0.59
	R^2	0.70	0.71	0.00	0.00	0.38	0.39	0.31	0.28	0.58	0.56
	p-value	7.43E-04	6.04E-04	9.45E-01	9.15E-01	3.29E-02	3.00E-02	5.95E-02	7.69E-02	4.00E-03	5.37E-03
	95% CI (Lower,Upper)	(1.35,3.71)	(0.57,1.51)	(-5.48,5.17)	(-2.08,1.90)	(0.01,0.13)	(0.00,0.05)	(-0.18,7.65)	(-0.19,3.07)	(0.23,0.91)	(0.08,0.37)
Climb PSF with	Formula	$C(t) = 12.65 - 3.07 * \sqrt{(t)}$	$C(t) = 15.94 + 1.30 * log(t)$	$C(t) = 27.10 - 0.79 * \sqrt{t}$	$C(t) = 27.89 + 0.21 * log(t)$	$C(t) = 0.15 + 0.02 * \sqrt{t}$	$C(t) = 0.13 - 0.01 * log(t)$	$C(t) = 37.41 - 8.04 * \sqrt{t}$	$C(t) = 45.92 + 3.18 * log(t)$	$C(t) = 5.62 - 0.38 * \sqrt{t}$	$C(t) = 6.04 + 0.18 * log(t)$
	Estimated k	3.07	1.30	0.79	0.21	-0.02	-0.01	8.03	3.18	0.38	0.18
	AIC	51.25	50.67	68.10	68.16	-36.74	-36.54	61.36	62.24	3.64	1.86
	R^2	0.34	0.37	0.01	0.00	0.03	0.01	0.60	0.57	0.29	0.39
	p-value	4.79E-02	3.65E-02	7.79E-01	8.57E-01	5.97E-01	7.25E-01	3.10E-03	4.56E-03	7.06E-02	3.04E-02
	95% CI (Lower,Upper)	(0.03,6.1)	(0.1,2.51)	(-5.33,6.91)	(-2.29,2.70)	(-0.10,0.06)	(-0.04,0.03)	(3.41,12.66)	(1.23,5.13)	(-0.04,0.80)	(0.02,0.34)
Road 1:20	Formula	$C(t) = 12.38 - 2.52 * \sqrt{t}$	$C(t) = 14.23 + 4.71 * log(t)$	$C(t) = 22.42 - 2.66 * \sqrt{t}$	$C(t) = 23.28 + 5.43 * log(t)$	$C(t) = 1.02 - 0.04 * \sqrt{t}$	$C(t) = 1.03 + 0.08 * log(t)$	$C(t) = 8.85 - 0.27 * \sqrt{t}$	$C(t) = 8.77 + 0.55 * log(t)$	$C(t) = 0.21 - 0.01 * \sqrt{t}$	$C(t) = 0.21 + 0.02 * log(t)$
	Estimated k	2.52	4.71	2.66	5.43	0.04	0.08	0.26	0.55	0.01	0.02
	AIC	157.50	155.83	178.29	172.18	2.94	-0.89	70.42	73.65	-31.24	-33.59
	R^2	0.76	0.78	0.53	0.64	0.31	0.41	0.46	0.37	0.13	0.21
	p-value	2.40E-08	1.11E-08	8.96E-05	5.08E-06	4.92E-03	7.58E-04	6.77E-04	3.18E-03	9.61E-02	2.75E-02
	95% CI (Lower,Upper)	(1.9,3.14)	(3.6,5.82)	(1.5,3.80)	(3.5,7.29)	(0.1,0.06)	(0.4,0.12)	(0.13,0.40)	(0.21,0.90)	(0.0,0.02)	(0.0,0.04)
Road 1:200	Formula	$C(t) = 6.16 - 1.29 * \sqrt{t}$	$C(t) = 6.73 + 2.54 * log(t)$	$C(t) = 6.42 - 0.98 * \sqrt{t}$	$C(t) = 6.38 + 2.09 * log(t)$	$C(t) = 0.14 - 0.01 * \sqrt{t}$	$C(t) = 0.15 + 0.03 * log(t)$	NA	NA	$C(t) = 0.62 + 0.03 * \sqrt{t}$	$C(t) = 0.35 + 0.03 * log(t)$
	Estimated k	1.29	2.54	0.98	2.09	0.01	0.03	NA	NA	-0.03	0.03
	AIC	172.34	166.09	184.15	173.79	-99.62	-107.11	NA	NA	25.72	25.81
	R^2	0.81	0.84	0.63	0.72	0.44	0.54	NA	NA	0.02	0.01
	p-value	2.86E-13	1.47E-14	1.58E-08	1.12E-10	7.54E-06	1.99E-07	NA	NA	7.32E-01	8.09E-01
	95% CI (Lower,Upper)	(1.07,1.52)	(2.14,2.93)	(0.71,1.25)	(1.63,2.55)	(0.01,0.02)	(0.02,0.03)	NA	NA	(-0.21,0.15)	(-0.28,0.34)
Road PSF without	Formula	$C(t) = 16.90 - 6.76 * \sqrt{t}$	$C(t) = 24.25 + 3.12 * log(t)$	$C(t) = 25.54 - 7.37 * \sqrt{t}$	$C(t) = 33.28 + 2.79 * log(t)$	$C(t) = 0.74 - 0.17 * \sqrt{t}$	$C(t) = 0.92 + 0.07 * log(t)$	NA	NA	$C(t) = 0.90 + 0.30 * \sqrt{t}$	$C(t) = 0.59 - 0.10 * log(t)$
	Estimated k	6.76	3.12	7.37	2.79	0.17	0.07	NA	NA	-0.30	-0.10
	AIC	66.45	63.79	69.39	70.40	-28.37	-30.78	NA	NA	3.70	4.55
	R^2	0.41	0.53	0.39	0.34	0.53	0.62	NA	NA	0.20	0.14
	p-value	2.50E-02	7.52E-03	2.92E-02	4.68E-02	7.10E-03	2.46E-03	NA	NA	1.45E-01	2.29E-01
	95% CI (Lower,Upper)	(1.04,12.48)	(1.04,5.2)	(0.91,13.83)	(0.05,5.53)	(0.06,0.28)	(0.03,0.11)	NA	NA	(-0.72,0.12)	(-0.28,0.07)
Road PSF with	Formula	$C(t) = 13.63 - 12.12 * \sqrt{t}$	$C(t) = 26.51 + 4.92 * log(t)$	$C(t) = 21.54 - 14.04 * \sqrt{t}$	$C(t) = 36.42 + 5.60 * log(t)$	$C(t) = 0.55 - 0.43 * \sqrt{t}$	$C(t) = 1.00 + 0.17 * log(t)$	$C(t) = 9.32 + 1.76 * \sqrt{t}$	$C(t) = 7.49 - 0.78 * log(t)$	$C(t) = 0.23 - 0.31 * \sqrt{t}$	$C(t) = 0.56 + 0.12 * log(t)$
	Estimated k	12.12	4.91	14.04	5.60	0.43	0.17	-1.76	-0.78	0.31	0.12
	AIC	66.17	66.43	73.85	74.57	-23.23	-19.81	11.99	12.41	-7.07	-6.78
	p-value	0.70	0.69	0.62	0.59	0.83	0.78	0.38	0.28	0.40	0.39
	R^2	7.44E-04	8.33E-04	2.44E-03	3.33E-03	3.58E-05	1.53E-04	5.80E-01	6.42E-01	2.65E-02	3.04E-02
	95% CI (Lower, Upper)	(6.47,17.77)	(2.58,7.23)	(6.26,21.82)	(2.34,8.86)	(0.29,0.57)	(0.11,0.23)	(-30.53,27.01)	(-16.58,15.02)	(0.04,0.58)	(0.01,0.23)

B. Leaching Plots

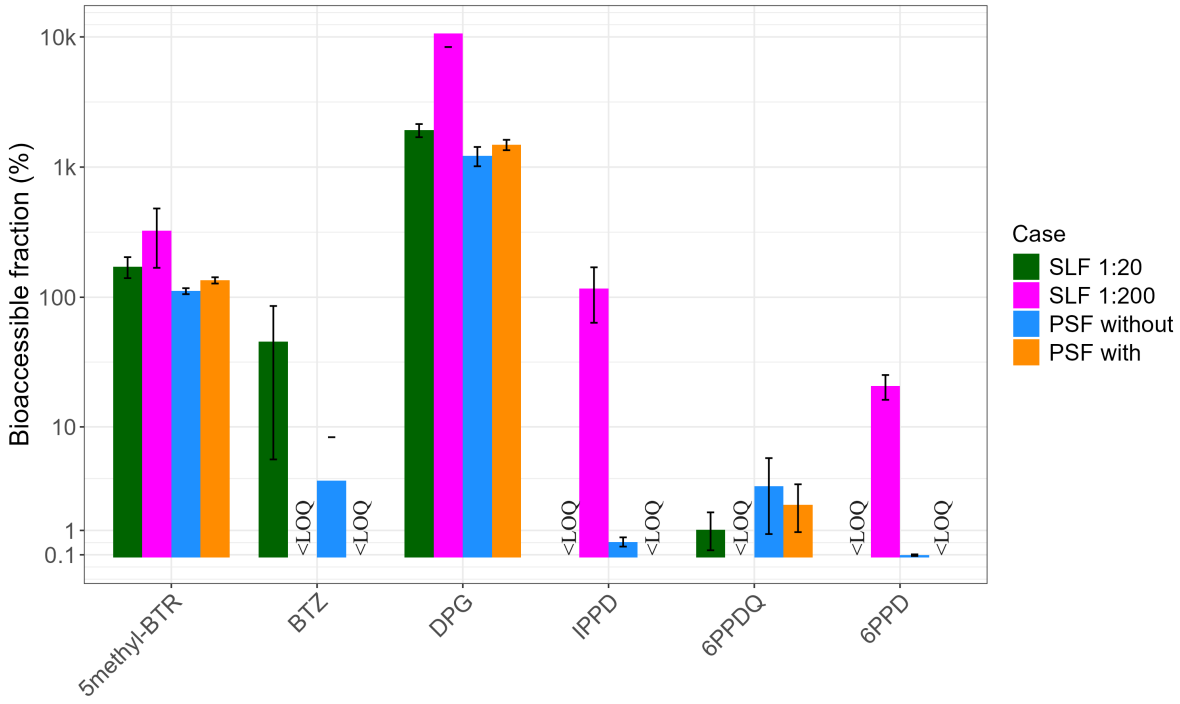

Figure B1.: Bioaccessible fractions for road dust.

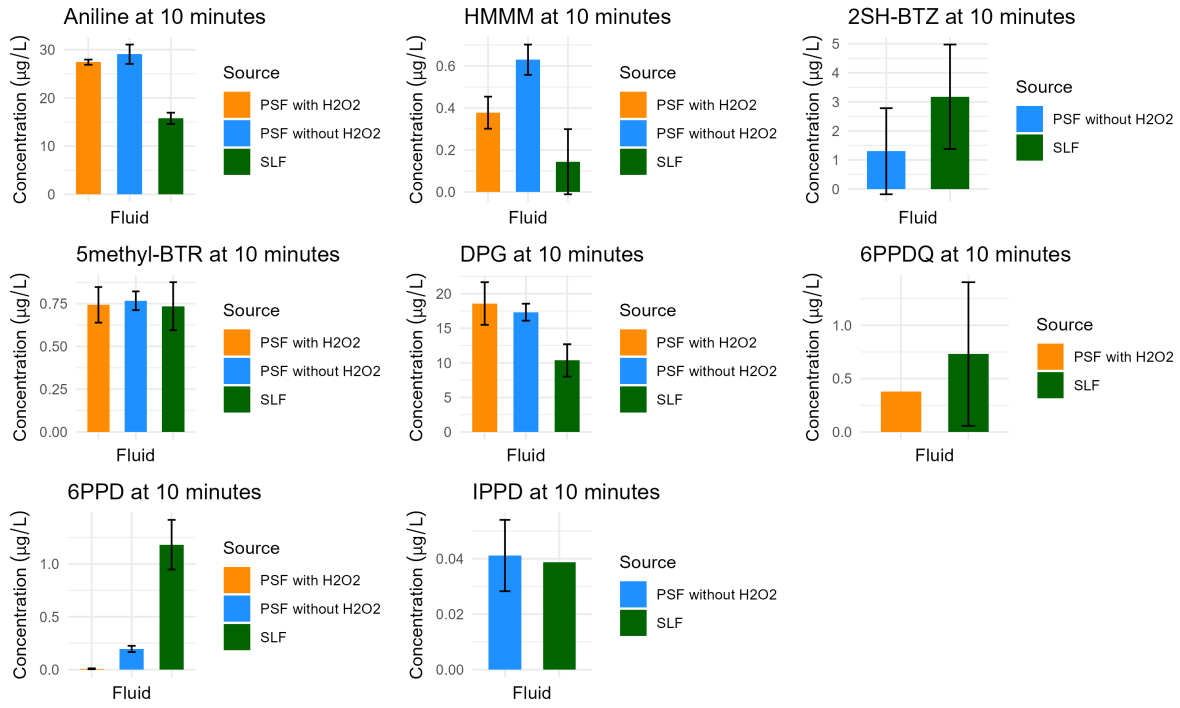

Figure B2.: Leaching after 0.17 hours in all fluids with road dust.

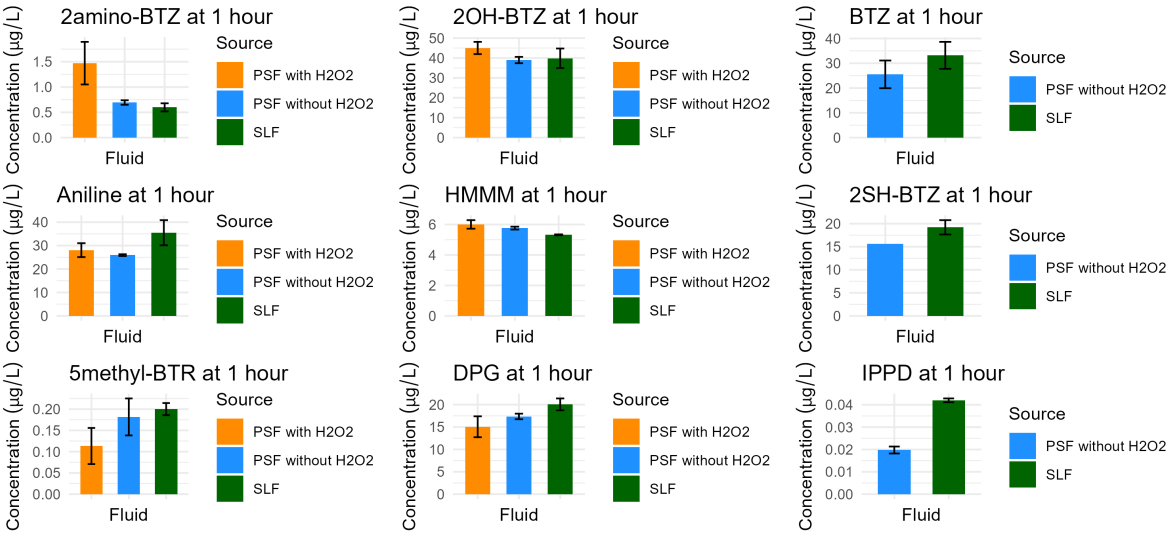

Figure B3.: Leaching after 1 hour in all fluids with climbing hall dust.

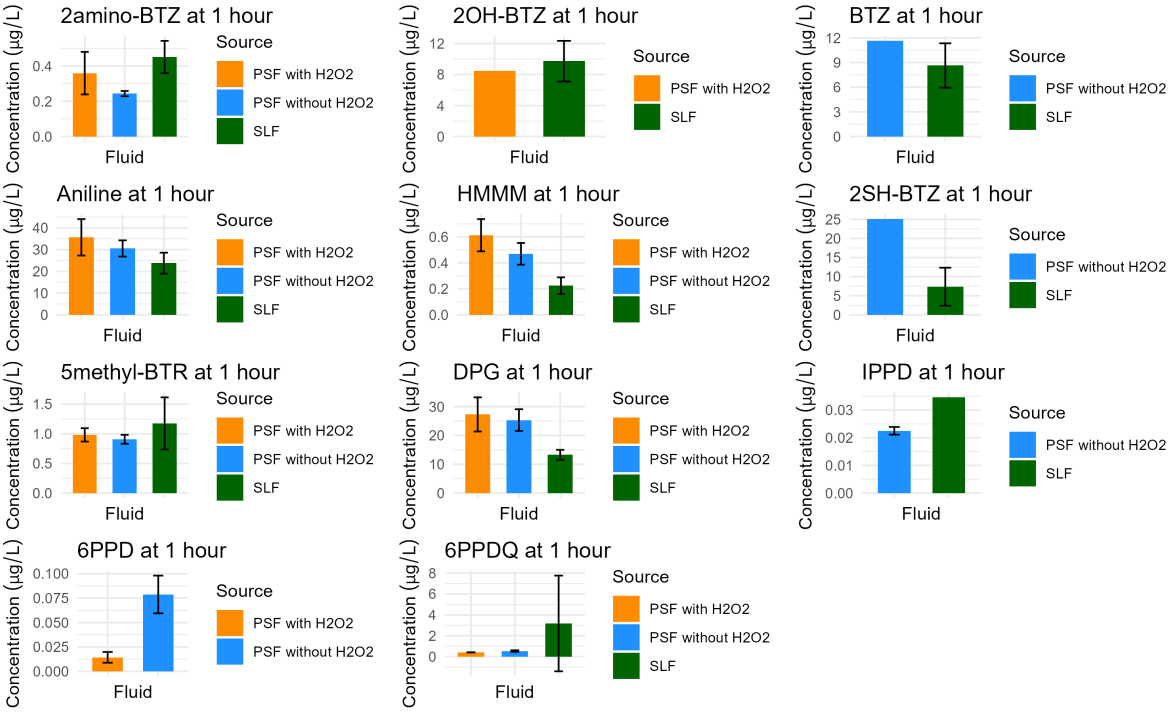

Figure B4.: Leaching after 1 hour in all fluids with road dust.

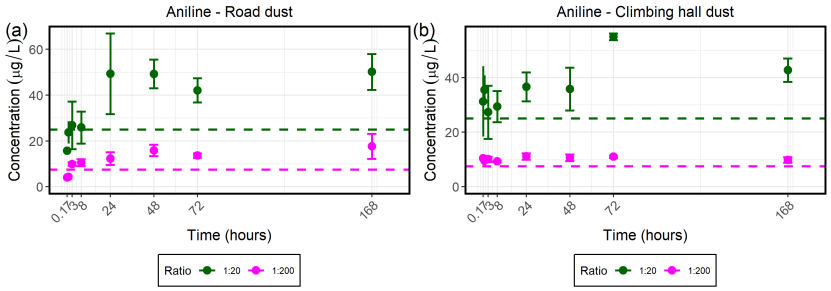

Figure B5.: Aniline Leaching in SLF for ratios 1:20 and 1:200 in (a) road dust and (b) for climbing hall dust.

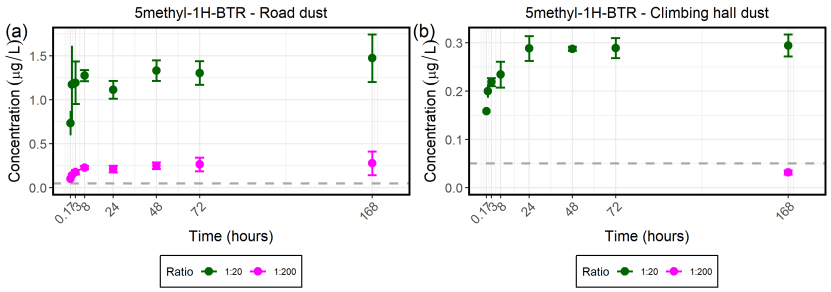

Figure B6.: 5methyl-BTR Leaching in SLF for ratios 1:20 and 1:200 in (a) road dust and (b) for climbing hall dust.

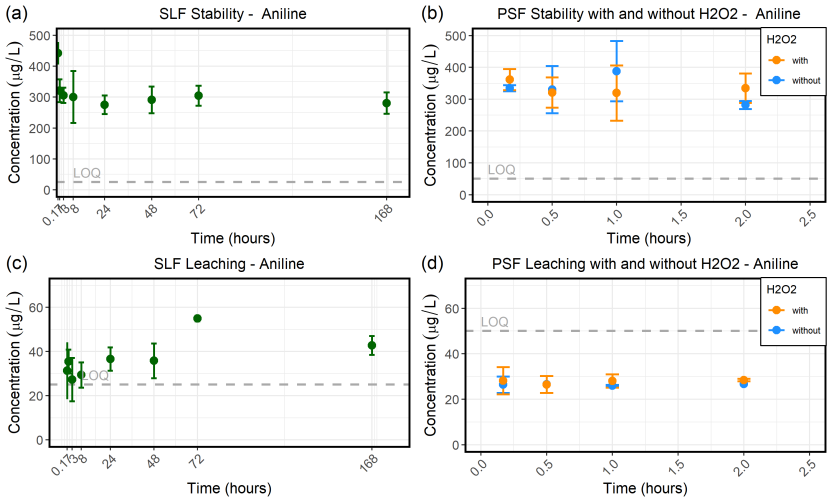

Figure B7.: Aniline Stability and Leaching in climbing hall dust.

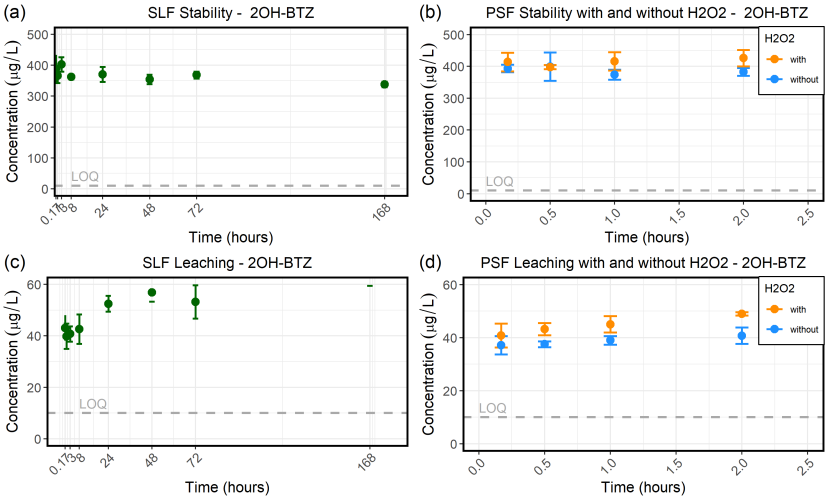

Figure B8.: 2OH-BTZ Stability and Leaching in climbing hall dust.

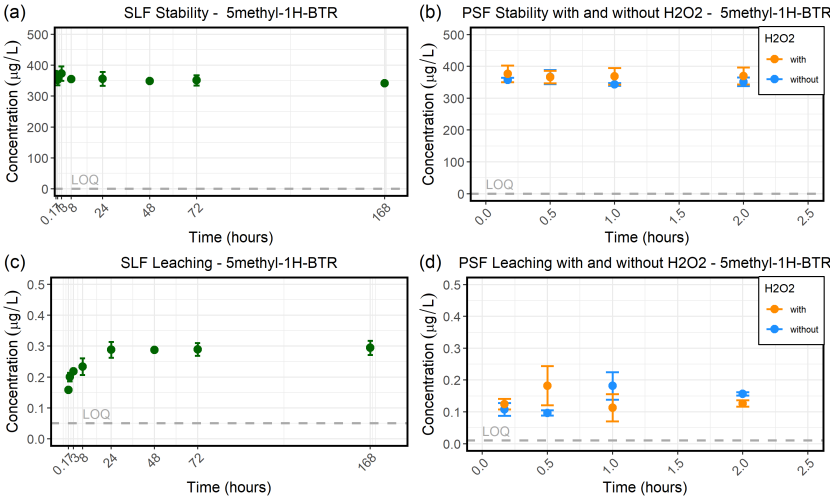

Figure B9.: 5methyl-BTR Stability and Leaching in climbing hall dust.

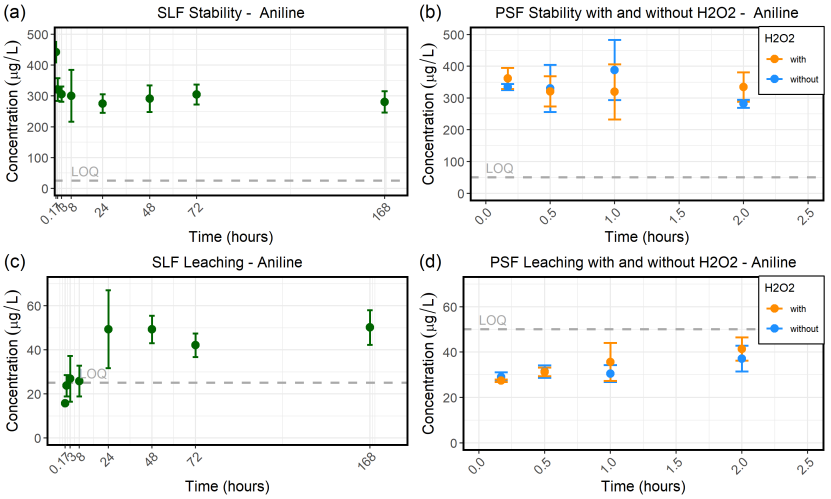

Figure B10.: Aniline Stability and Leaching in road dust.

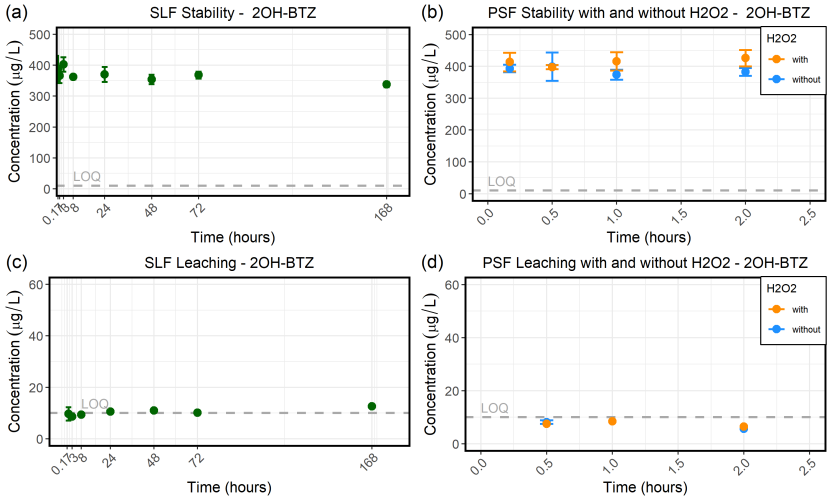

Figure B11.: 2OH-BTZ Stability and Leaching in road dust.

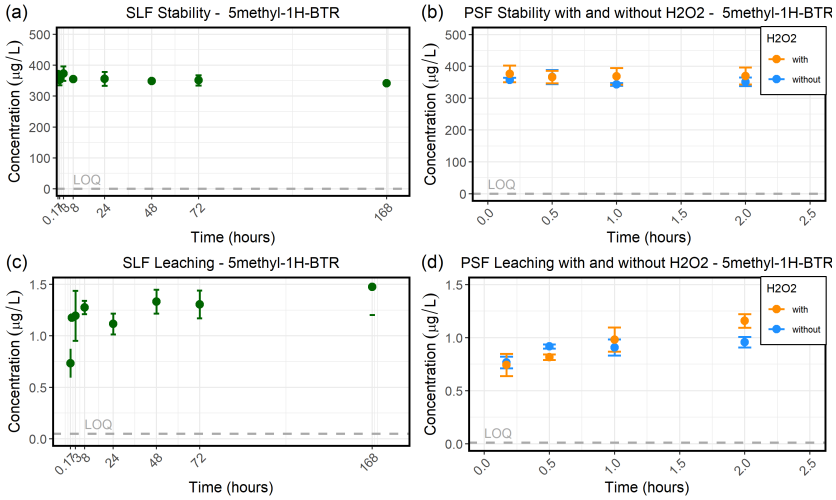

Figure B12.: 5methyl-BTR Stability and Leaching in road dust.

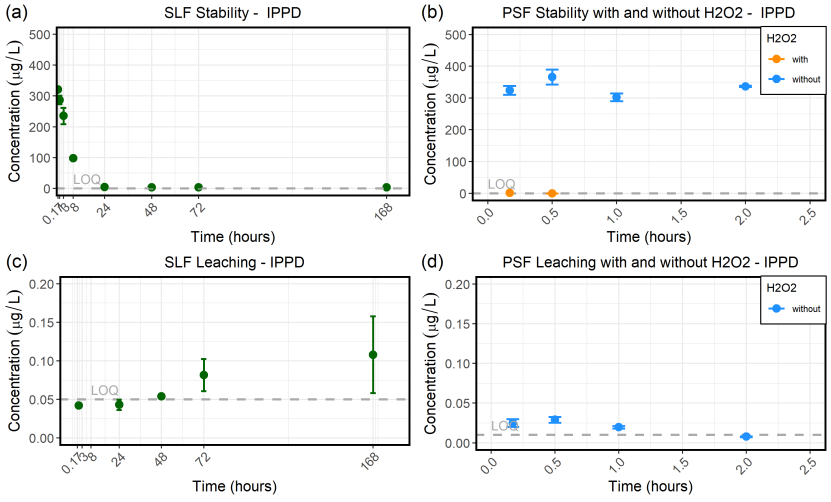

Figure B13.: IPPD Stability and Leaching in climbing hall dust.

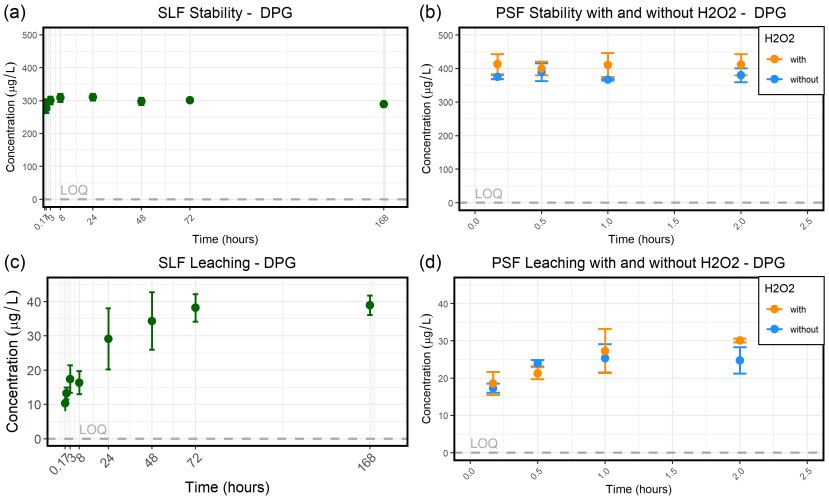

Figure B14.: DPG Stability and Leaching in road dust.

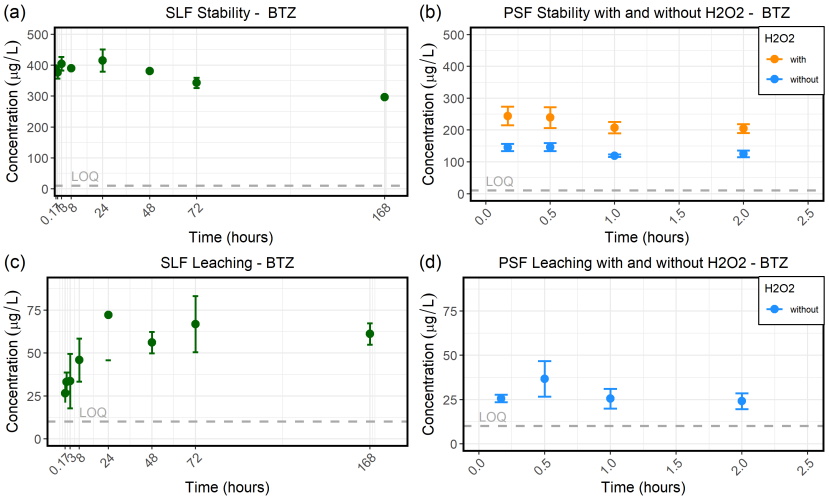

Figure B15.: BTZ Stability and Leaching in climbing hall dust.

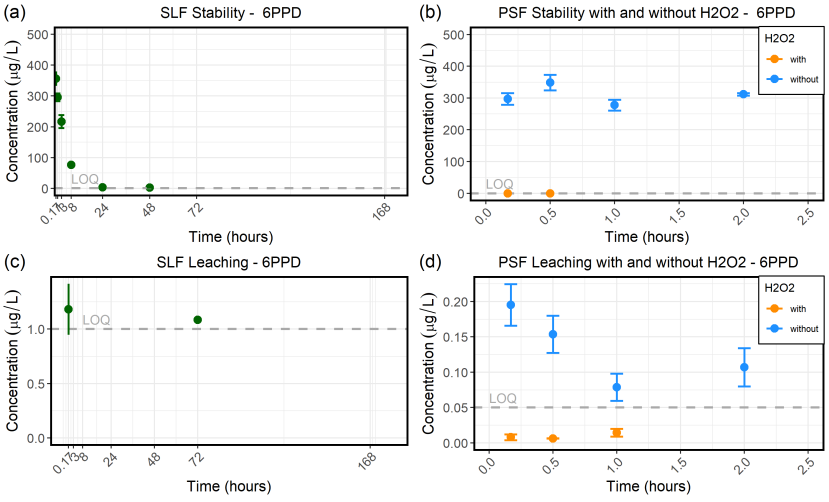

Figure B16.: 6PPD Stability and Leaching in road dust.

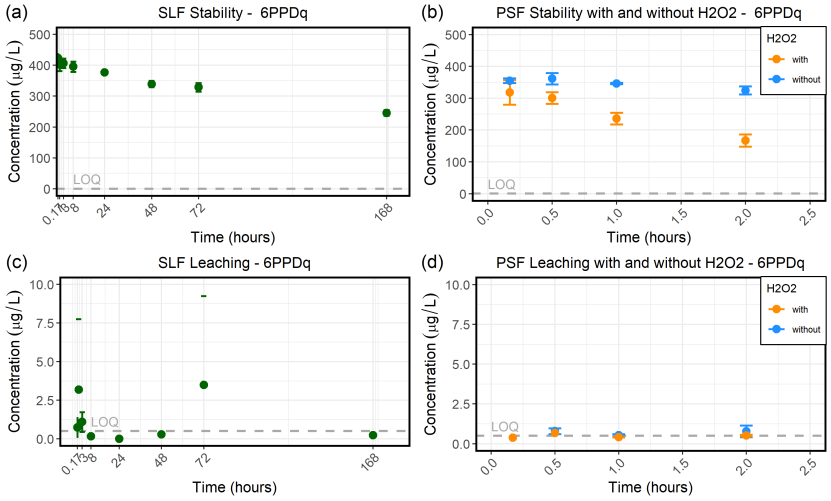

Figure B17.: 6PPDQ Stability and Leaching in road dust.

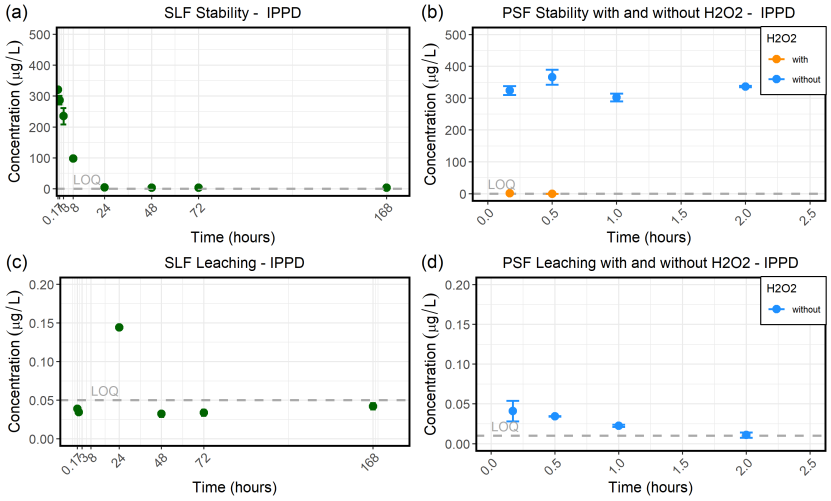

Figure B18.: IPPD Stability and Leaching in road dust.

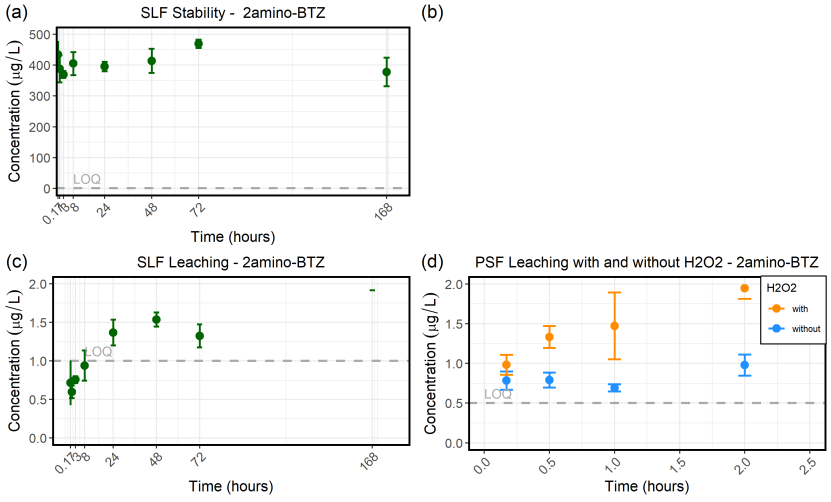

Figure B19.: 2amino-BTZ Stability and Leaching in climbing hall dust.

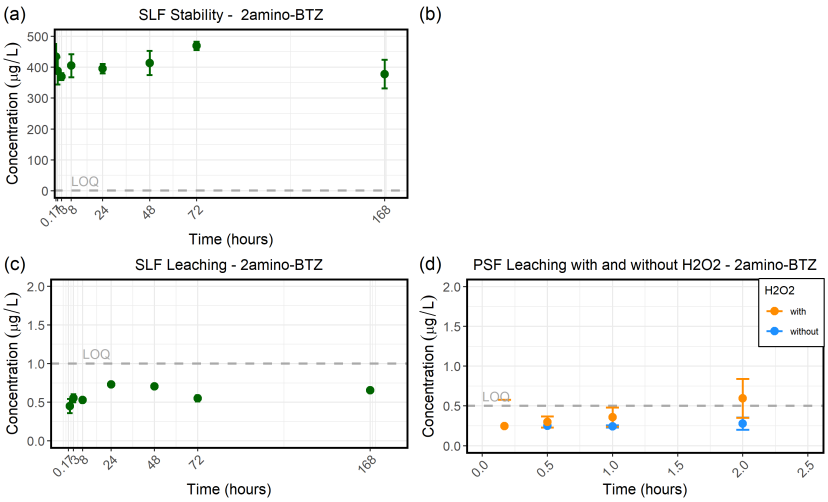

Figure B20.: 2amino-BTZ Stability and Leaching in road dust.

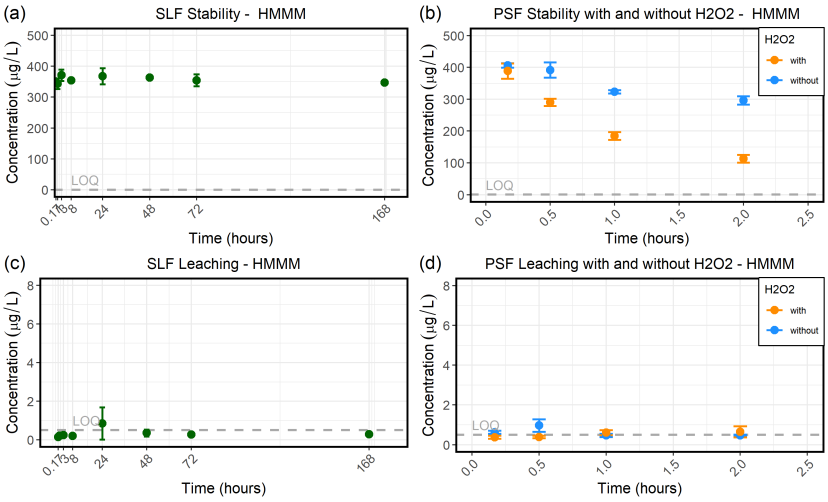

Figure B21.: HMMM Stability and Leaching in road dust.

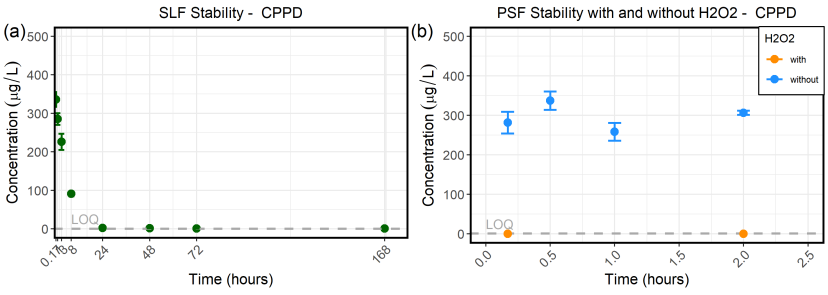

Figure B22.: CPPD Stability.

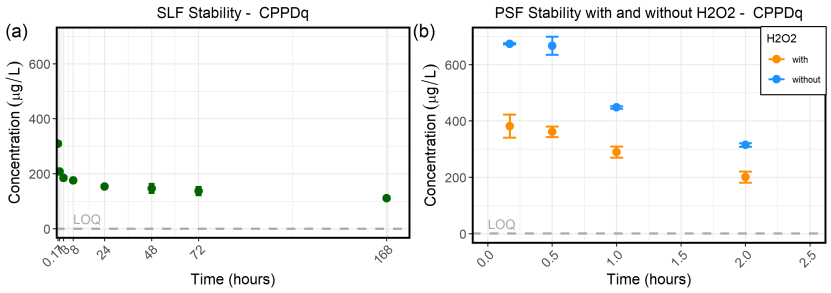

Figure B23.: CPPDQ Stability.

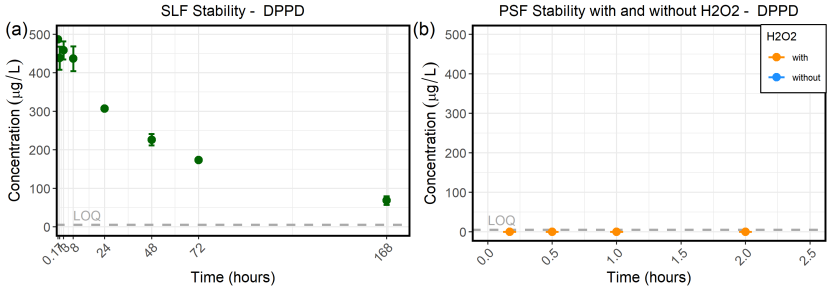

Figure B24.: DPPD Stability.

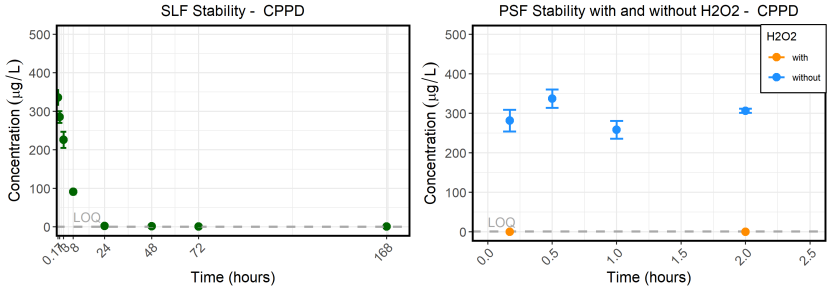

Figure B25.: DPPDQ Stability.

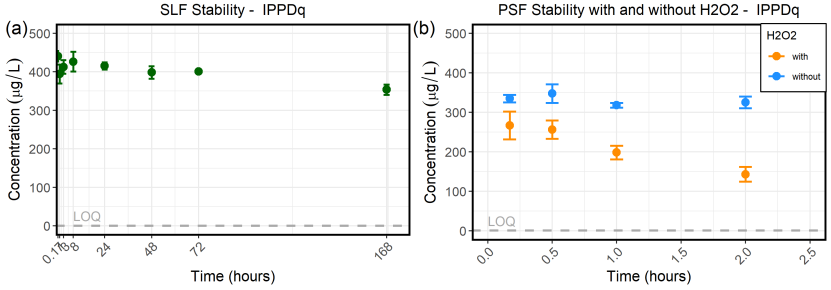

Figure B26.: IPPDQ Stability.